

# Tracer particle diffusion in a system with hardcore interacting particles

Simon Pigeon<sup>1,2,3</sup>, Karl Fogelmark<sup>3</sup>, Bo Söderberg<sup>3</sup>, Gautam Mukhopadhyay<sup>4,5</sup> and Tobias Ambjörnsson<sup>3</sup>

<sup>1</sup> Laboratoire Kastler Brossel, UPMC-Sorbonne Universités, CNRS, ENS-PSL Research University, Collège de France, 4 place Jussieu Case 74, F-75005 Paris, France.

<sup>2</sup> Centre for Theoretical Atomic, Molecular and Optical Physics, School of Mathematics and Physics, Queen's University Belfast, Belfast BT7 1NN, United Kingdom.

<sup>3</sup> Department of Astronomy and Theoretical Physics, Lund University, SE-223 62 Lund, Sweden.

<sup>4</sup> MU-DAE Centre for Excellence in Basic Science, Mumbai-400098, India.

<sup>5</sup> Physics Department, Indian Institute of Technology, Bombay, Powai, Mumbai 400076, India.

E-mail: [simon.pigeon@lkb.upmc.fr](mailto:simon.pigeon@lkb.upmc.fr)

**Abstract.** In this study, inspired by the work of K. Nakazato and K. Kitahara [*Prog. Theor. Phys.* **64**, 2261 (1980)], we consider the theoretical problem of tracer particle diffusion in an environment of diffusing hardcore interacting crowder particles. The tracer particle has a different diffusion constant from the crowder particles. Based on a transformation of the generating function, we provide an exact formal expansion for the tracer particle probability density, valid for any lattice in the thermodynamic limit. By applying this formal solution to dynamics on regular Bravais lattices we provide a closed form approximation for the tracer particle diffusion constant which extends the Nakazato and Kitahara results to include also b.c.c. and f.c.c. lattices. Finally, we compare our analytical results to simulations in two and three dimensions.

## Contents

<b>1</b>	<b>Introduction</b>	<b>2</b>
<b>2</b>	<b>Many-body expansion for arbitrary lattices</b>	<b>4</b>
2.1	Hardcore interacting particles on a lattice . . . . .	5
2.2	Mapping the system . . . . .	7
2.3	Thermodynamic limit . . . . .	8
2.4	Phase-rotated dynamics of $\tilde{\mathcal{L}}$ . . . . .	9
2.5	Expansion in terms of particle correlation functions . . . . .	10

<b>3</b>	<b>Crowding effects on tracer particle diffusion on regular lattices</b>	<b>12</b>
3.1	Mean square displacement on regular lattices . . . . .	13
3.2	Zeroth order: mean field approximation . . . . .	14
3.3	First order: including two-body correlation effects . . . . .	14
<b>4</b>	<b>Comparison with simulation results</b>	<b>16</b>
4.1	Simulations using the Gillespie algorithm . . . . .	16
4.2	Comparison between simulations and analytic predictions . . . . .	17
<b>5</b>	<b>Summary</b>	<b>19</b>
<b>Appendix A Phase rotation of the initial states</b>		<b>20</b>
<b>Appendix B Phase-rotated Liouvillian</b>		<b>21</b>
<b>Appendix C Two-body correlation function</b>		<b>22</b>
<b>Appendix D First order correlation factor: time dependence and long time limit</b>		<b>26</b>
<b>Appendix E Fitting procedure for the diffusion constant</b>		<b>27</b>

## 1. Introduction

Diffusion of a particle in a crowded environment is a classical problem in statistical physics. Among the different possible models, the simplest is to consider the motion of a tracer particle on a lattice surrounded by crowders at concentration  $c$ , see Fig. 1. In this model, which we explore herein,  $n$  random walkers, each jumping on a lattice of  $N$  sites in  $d$  dimensions, surround a diffusing single (tagged) tracer particle. The tracer particle has a jump rate  $r_T$  and each crowding particle has a jump rate  $r_C$ . Two particles cannot occupy the same lattice site (hardcore repulsion). It is intuitively clear from Fig. 1 that such crowding can severely change the effective diffusion of a tracer particle as compared to a freely diffusing particle (no crowding particles).

In the mean field approximation the reduction in the diffusion constant is obtained simply by counting the global average number of available sites for the tracer particle; the diffusion constant then is assumed to be reduced by a factor  $1 - c$ , where  $c = n/(N - 1)$  is the concentration of crowder particles. The mean field result is a good approximation when  $r_C \gg r_T$  in which case the tracer particle at every instance in time “experiences” a local crowder concentration equal to the global average. For the general case, it is convenient to extract the mean field result and write the tracer particle mean square displacement (MSD) for the crowded system as

$$\mathcal{MSD}(t) = 2dD_0t(1 - c)f(t, c, r_T, r_C), \tag{1}$$

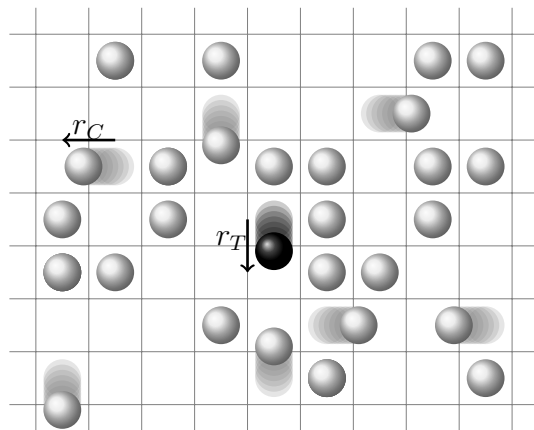


**Figure 1.** Schematic illustration of the dynamics of a tracer particle in crowded system. The dynamics takes place on a lattice where a set of crowder (white) particles attempt to move with jump rate  $r_C$ , and a tracer particle (black) attempts to move with jump rate  $r_T$ . The particles are subject to hard core repulsion, i.e. they cannot occupy the same site. We here investigate the asymptotic statistical properties of the tracer particle motion in such a scenario. Note that we here use a two-dimensional square lattice for illustrational purposes only – the results derived herein apply to regular Bravais lattices in arbitrary number of dimensions.

where  $D_0 = n_b a^2 r_T / (2d)$  corresponds to the diffusion constant of a single tracer particle in the absence of crowder particles. Above,  $n_b$  is the number of nearest neighbours on the lattice and  $a$  is the distance between such neighbours. The quantity  $f(t, c, r_T, r_C)$  is referred to as the correlation factor and it quantifies corrections to the mean field approximation. Thus, the correlation factor contains all remaining information of the diffusion constant's dependence on the underlying physical parameters, namely  $r_T$ ,  $r_C$  and  $c$  and on the lattice geometry. To illustrate the origin of the correlation factor, consider e.g. that the tracer particle is attempting to jump to a site occupied by a crowder particle. This move will be prohibited due to the hardcore interaction. However, at the next time step the tracer particle can attempt to jump to the same site. If the jump rate of the crowder particle is such that  $r_C/r_T \ll 1$  it is probable that the same crowder particle will inhibit this move once more. This type of two-body correlation effect is not incorporated in the mean field approximation and, as we will show, in general, leads to  $f(t, c, r_T, r_C) < 1$ .

Both the generality and complexity of the problem make its exact resolution very challenging, if not impossible [1]. Most of the existing literature focus on specific cases. For example, if crowder particles do not move ( $r_C = 0$ ) one has a single tagged particle moving stochastically in a statically disordered medium [2, 3] (percolation). Another well explored related scenario corresponds to single file diffusion [4], where in a linear lattice each particle with identical jump rate ( $r_C = r_T$ ) diffuse sub-linearly with time. Moreover, diffusion of a forced tagged particle in a crowded lattice is an actively explored problem [5, 6, 7, 8, 9]. Some specific lattice structures were studied also, such as stripes and capillaries [10], presenting rich scaling behavior.

For the general case considered here (arbitrary concentration and particle jump rates) only a few approximation schemes were proposed [11, 12, 13, 14, 15, 16]. More significant results were obtained by Tahir-Kheli and Elliott [17] based on a decoupling scheme of many-particle correlation functions. The same results were expressed in terms of the velocity autocorrelation function by van Beijeren and Kutner [18]. Some interesting results were more recently obtained in the limit of high concentration [19, 20] for forced tagged particle motion [21, 22, 23].

In our work, we provide all details of derivation of the transformed (phase-rotated) Liouvillian operator introduced by Nakazato and Kitahara [15]. To our knowledge, this full explicit derivation has not been provided before. We then rigorously derive the thermodynamic limit for the tracer particle probability density function (PDF). Based on this PDF we obtain an exact expansion of the correlation factor,  $f(t, c, r_T, r_C)$ , in terms of  $n$ -body correlation functions, which is independent of the network or lattice structure. By calculating the first order term in the formal expansion we extend Nakazato and Kitahara's results [15] (valid for linear, square and cubic lattices) to also include b.c.c. and f.c.c. lattices. Through extensive simulations we further study in detail the limitation of our first-order approximation. Our simulation software package is made publically available. Since our theoretical results are grounded in a formally exact result, it opens up for future systematic improvements of our approximations.

The structure of this article is as follows: in Sec. 2, we provide an exact expansion, in terms of many-body correlation functions, for the probability density function (PDF) for the tracer particle position in a crowded environment, valid for arbitrary lattice geometries (Sec. 2.1). We then present the mathematical mapping used in this study (Sec. 2.2) and derive an expression for the PDF in the thermodynamic limit (Sec. 2.3). We then discuss the dynamics in the mapped system (Sec. 2.4) and present a formal many-body expansion (Sec. 2.5). The next Sec. 3 focuses on dynamics for regular lattices. For these lattices, translation invariance allows a derivation of different terms in the proposed expansion (Sec. 3.1). We then consider the zeroth order of the expansion (Sec. 3.2), followed by the determination of the crowding effect to the first order (Sec. 3.3). In the final Sec. 4, we compare the derived results to simulations for each of the lattices (in two and three dimensions) considered.

## 2. Many-body expansion for arbitrary lattices

In this section we will focus on the general mathematical formalism and derivations for general lattice geometries. After some definitions using the Dirac bra-ket notation (Sec. 2.1) we map the system (Sec. 2.2) and derive an expression for the PDF in the thermodynamic limit (Sec. 2.3). It is followed by more details on the mapped system dynamics (Sec. 2.4) and our expansion for the PDF of the tracer particle in terms of a sum of contributions from  $n$  crowder particle correlations (Sec. 2.5). The derivations in Secs. 2.2-2.4 follow closely those of Ref. [15], but are here provided in a slightly expanded format for completeness.

### 2.1. Hardcore interacting particles on a lattice

We consider a simple lattice of  $N$  lattice sites in  $d$  dimensions. Each site is defined by a position vector  $\mathbf{u}$ . Although we will use square lattices to illustrate the system behavior and our mapping, what follows in this section is independent of the lattice nature. The lattice contains one tracer particle and  $n$  crowder particles. A given microscopical state of the system is thus fully characterized by the tracer particle position,  $\mathbf{r}$ , and crowder particle positions,  $\mathbf{r}_i$  with  $i = \{1, \dots, n\}$ . We use the bra-ket notation to define the states and the dynamics of the system. For example, a state of the system where only the tracer particle is present and located at position  $\mathbf{r}$  is denoted as:

$$|T_{\mathbf{r}}\rangle \cdot \underbrace{\left( \prod_{\substack{i=1 \\ \mathbf{u}_i \neq \mathbf{r}}}^N |0_{\mathbf{u}_i}\rangle \right)}_{|\{\emptyset\}\rangle} \quad (2)$$

where  $|0_{\mathbf{u}_i}\rangle$  is a local state corresponding to no particle at site  $\mathbf{u}_i$ . A local site state with a tracer particle present at position  $\mathbf{r}$  is denoted by  $|T_{\mathbf{r}}\rangle$ . A general allowed state with both tracer and crowsers present is written as the (direct) product of all  $N$  local states according to

$$|T_{\mathbf{r}}\rangle \cdot \left( \prod_{i=1}^n |C_{\mathbf{r}_i}\rangle \right) \cdot |\{\emptyset\}\rangle \quad (3)$$

where it is understood that  $\mathbf{r}$  and all  $\mathbf{r}_i$  are distinct, and where  $|\{\emptyset\}\rangle$  denotes remaining (non-occupied) sites, i.e., the product of local states with neither tracer nor crowder particles. Local crowder particle states are denoted by  $|C_{\mathbf{r}_i}\rangle$ . We use the following orthogonality rule [15]

$$\langle X_{\mathbf{r}} || Y_{\mathbf{r}} \rangle = \delta_{X,Y}, \quad (4)$$

where  $X$  and  $Y$  each represents one of the three types of lattice states we consider:  $T$  for tracer particle,  $C$  for crowder particle or  $0$  for an empty site. This orthogonality relation, together with our explicit form for the Liouvillian below, handles the hardcore repulsion, forbidding two particles to occupy the same site on the lattice. The completeness relation becomes:

$$I = \sum_{n=0}^{N-1} \sum_{\substack{\mathbf{r}, \mathbf{r}_1, \dots, \mathbf{r}_n \\ \mathbf{r}_i \neq \mathbf{r} \\ \mathbf{r}_i \neq \mathbf{r}_j}} |T_{\mathbf{r}}\rangle |C_{\mathbf{r}_1}\rangle \cdots |C_{\mathbf{r}_n}\rangle |\{\emptyset\}\rangle \langle\{\emptyset\}| \langle C_{\mathbf{r}_n} | \cdots \langle C_{\mathbf{r}_1} | \langle T_{\mathbf{r}} | \quad (5)$$

where the sums run over all allowed crowder and tracer particle configurations (crowder particles are indistinguishable). The quantity  $I$  above is an identity operator which when applied to any lattice state leaves that state unchanged. Notice, however, the constraints in the sum above, which guarantee that particles cannot occupy the same lattice site.

Let us now consider the dynamics. For a given particle type  $P$  ( $P = T$  for tracer or  $C$  for crowder) we define an update operator according to

$$\mathcal{U}_P = \sum_{i=1}^N \sum_{\mathbf{b}} \left( |P_{\mathbf{u}_i+\mathbf{b}}\rangle \langle 0_{\mathbf{u}_i+\mathbf{b}}| |0_{\mathbf{u}_i}\rangle \langle P_{\mathbf{u}_i}| - |P_{\mathbf{u}_i}\rangle \langle P_{\mathbf{u}_i}| |0_{\mathbf{u}_i+\mathbf{b}}\rangle \langle 0_{\mathbf{u}_i+\mathbf{b}}| \right). \quad (6)$$

There are two sums above. The first sum is over all sites of the lattice. The second sum is over all neighboring sites of site  $\mathbf{u}_i$ , where the quantity  $\mathbf{b}$  is a displacement vector to a nearest neighbor site. Within the sums there are two terms. The first term corresponds to a scenario where a particle of type  $P$  on a site  $\mathbf{u}_i$  is replaced by an empty site ( $P$  particle annihilated) followed by the creation of a  $P$  particle in  $\mathbf{u}_i + \mathbf{b}$ , if that site is empty. This first term is thus a moving operator. With the orthogonality relation we defined in Eq. (4) it is clear that the moving operator is only effective if a  $P$  particle is present in  $\mathbf{u}_i$  and if the site  $\mathbf{u}_i + \mathbf{b}$  is empty, thus making sure that the hardcore constraint is satisfied. The second term is negative and contains the projection operator onto states with a  $P$  particle at  $\mathbf{u}_i$  and an empty site at  $\mathbf{u}_i + \mathbf{b}$ . These two terms signify that in a small time window a particle can either jump (first term) or remain at its current position (second term). Fig. 2 schematically illustrates the superposition of eight states produced by the action of the operator  $\mathcal{U}_P$  on a square lattice containing a single  $P$  particle.

$$\mathcal{U}_P \left| \begin{array}{c} \square \\ \square \\ \square \end{array} \right\rangle = \left| \begin{array}{c} \square \\ \square \\ \square \end{array} \right\rangle + \left| \begin{array}{c} \square \\ \square \\ \square \end{array} \right\rangle + \left| \begin{array}{c} \square \\ \square \\ \square \end{array} \right\rangle + \left| \begin{array}{c} \square \\ \square \\ \square \end{array} \right\rangle + \left| \begin{array}{c} \square \\ \square \\ \square \end{array} \right\rangle - 4 \left| \begin{array}{c} \square \\ \square \\ \square \end{array} \right\rangle$$

**Figure 2.** Illustration of the action of the update operator  $\mathcal{U}_P$ , Eq. (6), applied to a square lattice with one particle  $P$ .

For the simplest case of a single tracer particle in the absence of crowders, the probability density function (PDF) of finding the particle in a position  $\mathbf{r}$  starting from  $\mathbf{r}_0$  at time  $t$  is

$$P(\mathbf{r}, t | \mathbf{r}_0) = \langle \{\emptyset\} | \langle T_{\mathbf{r}} | e^{tr_T \mathcal{U}_T} | T_{\mathbf{r}_0} \rangle | \{\emptyset\} \rangle, \quad (7)$$

where  $r_P$  represents the jump rate of a  $P$  particle for passing to a nearest neighbour site. This is the PDF for a single random walker on a lattice.

Our interest focuses on the diffusion of a tracer particle in a crowded system with  $n$  crowder particles. The PDF for finding the tracer particle at position  $\mathbf{r}$  after a time

$t$ , given an initial position  $\mathbf{r}_0$ , then is:

$$P_{n,N}(\mathbf{r}, t|\mathbf{r}_0) = \frac{1}{\binom{N-1}{n}} \langle\{\emptyset\}|\langle T_{\mathbf{r}}| \sum_{\mathbf{r}_1, \dots, \mathbf{r}_n} \langle C_{\mathbf{r}_1} | \dots \langle C_{\mathbf{r}_n} |$$

$$\times e^{t\mathcal{L}} \sum_{\mathbf{r}'_1, \dots, \mathbf{r}'_n} |C_{\mathbf{r}'_1}\rangle \dots |C_{\mathbf{r}'_n}\rangle |T_{\mathbf{r}_0}\rangle |\{\emptyset\}\rangle \quad (8)$$

where  $\sum_{\mathbf{r}_1, \dots, \mathbf{r}_n}$  represents the sum over all the possible configurations of the  $n$  crowder particles on the  $N - 1$  sites (thermal initial condition). The dynamics of our system is determined by the Liouvillian operator  $\mathcal{L} = r_C \mathcal{U}_C + r_T \mathcal{U}_T$ , which allows either the crowder particles to move with a rate  $r_C$  or the tracer particle to move with a rate  $r_T$  at any given instant. Due to the hardcore repulsion, care is required when calculating Eq. (8). Formally, this expression can be evaluated by dividing time into small time slices, i.e. we write  $\exp(t\mathcal{L}) = \prod_{k=1}^K \mathcal{O}_k$  with  $\mathcal{O}_k = \exp[\epsilon_k \mathcal{L}]$  and  $\epsilon_k = t_k - t_{k-1}$ , with  $t_K = t$  and  $t_0 = 0$ . Between each  $\mathcal{O}_k$ -operator in the product above, one then inserts completeness relations, see Eq. (5). Such an approach (for  $\epsilon_k \rightarrow 0$ ) ensures that at no time in  $[0, t]$  do any two particles occupy the same lattice site. Due to the constraints imposed in Eq. (5) such an approach is not practical, however. Instead, we here introduce a transformation which allows us to rewrite the PDF above in terms of few-body states (to lowest orders in an expansion). When the number of particles is one or two in the transformed domain, we can deal with the hardcore repulsion by introducing absorbing conditions for the many-body propagator.

## 2.2. Mapping the system

Following Ref. [15] we now define the following generating function:

$$G(\mathbf{r}, t|\mathbf{r}_0; x) = \sum_{n=1}^N x^n P_{n,N}(\mathbf{r}, t|\mathbf{r}_0) \binom{N-1}{n} \quad (9)$$

where  $P_{n,N}(\mathbf{r}, t|\mathbf{r}_0)$  is given in Eq. (8). The binomial coefficient in the definition of the generating function corresponds to the number of ways of placing the  $n$  indistinguishable crowder particles on  $N - 1$  sites (one of the  $N$  sites is occupied by the tracer particle). We will later find it useful to normalize this generating function according to:

$$g(\mathbf{r}, t|\mathbf{r}_0; x) = \frac{1}{(1+x)^{N-1}} G(\mathbf{r}, t|\mathbf{r}_0; x). \quad (10)$$

Using Eqs. (8) and (9) we have that [15]

$$G(\mathbf{r}, t|\mathbf{r}_0; x) = \langle\{\emptyset\}|\langle T_{\mathbf{r}}| \prod_{\substack{i=1 \\ \mathbf{u}_i \neq \mathbf{r}}}^N \left(1 + \sqrt{x} |0_{\mathbf{u}_i}\rangle \langle C_{\mathbf{u}_i}|\right) e^{t\mathcal{L}} \prod_{\substack{j=1 \\ \mathbf{u}_j \neq \mathbf{r}_0}}^N \left(1 + \sqrt{x} |C_{\mathbf{u}_j}\rangle \langle 0_{\mathbf{u}_j}|\right) |T_{\mathbf{r}_0}\rangle |\{\emptyset\}\rangle. \quad (11)$$

The equivalence of Eqs. (8) and (9) to Eq. (11) follows directly by explicitly writing out all terms in Eq. (11). We require that  $\mathbf{u}_i \neq \mathbf{r}$  and  $\mathbf{u}_j \neq \mathbf{r}_0$ , which above corresponds

to the requirement that no crowder particle can be placed on the same site as the tracer particle. Following Ref. [15], we apply a transformation (phase rotation) using the operator  $\mathcal{S}_{\mathbf{u}_i} = |C_{\mathbf{u}_i}\rangle\langle 0_{\mathbf{u}_i}| - |0_{\mathbf{u}_i}\rangle\langle C_{\mathbf{u}_i}|$ . Applying  $e^{-\theta \sum_{i=1}^N \mathcal{S}_{\mathbf{u}_i}}$ , with a phase parameter  $\theta$ , to the superposition of initial states (see Appendix A) we find that the generating function (10) can be conveniently written as

$$g(\mathbf{r}, t | \mathbf{r}_0; x) = \langle \{\emptyset\} | \langle T_{\mathbf{r}} | e^{t\check{\mathcal{L}}(\theta)} | T_{\mathbf{r}_0} \rangle | \{\emptyset\} \rangle \quad (12)$$

provided we choose  $\sqrt{x} = \tan \theta$ . The transformed Liouvillian is given by

$$\check{\mathcal{L}}(\theta) = e^{-\theta \mathcal{S}} \mathcal{L} e^{\theta \mathcal{S}}. \quad (13)$$

Thus, the phase rotation provides means for passing from a situation with a large number of initial and final states (more precisely,  $\binom{N-1}{n}$  states, see Eq. (8)) to a situation with only one initial and one final state. The final and initial states contain no crowder particles and only one tracer particle. This reduction, however, comes at the expense of a more complicated Liouvillian,  $\check{\mathcal{L}}(\theta)$ .

### 2.3. Thermodynamic limit

We now seek to derive a general expression for the tracer particle's PDF in the thermodynamic limit in terms of the phase-rotated generating function derived in the previous subsection. To that end, let us write Eqs. (9) and (10) according to:

$$g(\mathbf{r}, t | \mathbf{r}_0; x) = \sum_{n=1}^N F_N(n, x) P_c(\mathbf{r}, t | \mathbf{r}_0), \quad (14)$$

where

$$F_N(n, x) = \frac{x^n}{(1+x)^{N-1}} \binom{N-1}{n}. \quad (15)$$

In the limit of large  $N$  we have that  $F_N(n, x)$  converges to a normal distribution, i.e.,

$$\lim_{N \rightarrow \infty} F_N(n, x) = \frac{1}{\sqrt{2\pi\sigma^2}} \exp\left(-\frac{(n - \tilde{n})^2}{2\sigma^2}\right), \quad (16)$$

with  $\tilde{n} = Nx/(1+x)$  and  $\sigma^2 = Nx/(1+x)$ . Taking the thermodynamic limit, i.e. taking  $n$  to infinity with the concentration  $c = n/N$  kept fixed, we have:

$$\lim_{\substack{N \rightarrow \infty \\ n \rightarrow \infty \\ \text{with } n/N=c}} F_N(n, x) = \frac{1}{N} \delta\left(c - \frac{x}{(1+x)}\right). \quad (17)$$

Consequently, in the thermodynamic limit we choose

$$x = \frac{c}{1-c}. \quad (18)$$



Thus, in the thermodynamic limit the PDF becomes

$$p_c(\mathbf{r}, t|\mathbf{r}_0) = \lim_{\substack{N \rightarrow \infty \\ n \rightarrow \infty \\ \text{with } n/N=c}} P_{n,N}(\mathbf{r}, t|\mathbf{r}_0) = g(\mathbf{r}, t|\mathbf{r}_0; x = \frac{c}{1-c}), \quad (19)$$

where  $g(\mathbf{r}, t|\mathbf{r}_0; x)$  is given in Eq. (10). We consequently have equality between the thermodynamic limit PDF of a tracer particle moving through an environment of crowder particles (undergoing usual displacement and hard core repulsion:  $\mathcal{L}$ ) and the PDF of a tracer particle moving without crowder particles around and described by the modified Liouvillian  $\check{\mathcal{L}}(\theta)$ . Using Eq. (12) we write Eq. (19) on the final form

$$p_c(\mathbf{r}, t|\mathbf{r}_0) = \langle \{\emptyset\} | \langle T_{\mathbf{r}} | e^{t\check{\mathcal{L}}(\theta)} | T_{\mathbf{r}_0} \rangle | \{\emptyset\} \rangle \quad (20)$$

where the phase angle is determined by  $\theta = \arctan[\sqrt{x}] = \arctan[\sqrt{c/(1-c)}]$ . Equation Eq. (20) gives the probability to find the tracer particle at  $\mathbf{r}$  starting from  $\mathbf{r}_0$ , after a time  $t$ , in the thermodynamic limit knowing it is surrounded by a given concentration  $c$  of crowder particle (thermal initial conditions). Notice that the result above is independent of the geometry of the lattice, making it a powerful method to unravel crowding effect in complex lattices and networks as well as in regular lattices. The transformation is similar to a Lang–Firsov (polaron) transformation used for electronic system [24, 25].

#### 2.4. Phase-rotated dynamics of $\check{\mathcal{L}}$

Let us now investigate further the dynamics described by the Liouvillian  $\check{\mathcal{L}}(\theta)$ , see equation Eq. (13). This operator can be written (see Appendix B and Ref. [15])

$$\check{\mathcal{L}}(\theta) = r_C \mathcal{U}_C + r_T \cos^2 \theta \mathcal{U}_T + r_T \sin^2 \theta \mathcal{R} + r_T \cos \theta \sin \theta (\mathcal{C} + \mathcal{C}^\dagger), \quad (21)$$

where, in the thermodynamic limit, we have  $\cos^2 \theta \rightarrow (1-c)$ ,  $\sin^2 \theta \rightarrow c$  and  $\cos \theta \sin \theta \rightarrow \sqrt{c(1-c)}$  (because we have  $\sqrt{x} = \tan \theta$ ). The two first operators above were already formally defined through Eq. (6). The operator  $\mathcal{R}$  acts by exchanging the position of neighbor tracer and crowder particles:

$$\mathcal{R} = \sum_{i=0}^N \sum_{\mathbf{b}} \left( |T_{\mathbf{u}_i}\rangle \langle C_{\mathbf{u}_i} | | C_{\mathbf{u}_i+\mathbf{b}} \rangle \langle T_{\mathbf{u}_i+\mathbf{b}} | - |T_{\mathbf{u}_i}\rangle \langle T_{\mathbf{u}_i} | | C_{\mathbf{u}_i+\mathbf{b}} \rangle \langle C_{\mathbf{u}_i+\mathbf{b}} | \right). \quad (22)$$

Finally, the non-conservative operators  $\mathcal{C}$  and  $\mathcal{C}^\dagger$  are more “exotic” in the sense that they do not conserve the number of crowder particles. These operators annihilate or create a crowder particle close to a tracer particle, respectively.

$$\mathcal{C}^\dagger = \sum_{i=0}^N \sum_{\mathbf{b}} \left( |T_{\mathbf{u}_i}\rangle \langle T_{\mathbf{u}_i} | | C_{\mathbf{u}_i+\mathbf{b}} \rangle \langle 0_{\mathbf{u}_i+\mathbf{b}} | - |T_{\mathbf{u}_i}\rangle \langle 0_{\mathbf{u}_i} | | C_{\mathbf{u}_i+\mathbf{b}} \rangle \langle T_{\mathbf{u}_i+\mathbf{b}} | \right), \quad (23)$$

$$\mathcal{C} = \sum_{i=0}^N \sum_{\mathbf{b}} \left( |T_{\mathbf{u}_i}\rangle \langle T_{\mathbf{u}_i} | | 0_{\mathbf{u}_i+\mathbf{b}} \rangle \langle C_{\mathbf{u}_i+\mathbf{b}} | - |T_{\mathbf{u}_i}\rangle \langle C_{\mathbf{u}_i} | | 0_{\mathbf{u}_i+\mathbf{b}} \rangle \langle T_{\mathbf{u}_i+\mathbf{b}} | \right). \quad (24)$$

Here the  $\mathcal{C}^\dagger$  operator takes effect only when applied to states with a tracer particle close to an empty site (like  $\mathcal{U}_T$ ), while the operator  $\mathcal{C}$  takes effect only when applied to states with a crowder particle close to the tracer particle (like  $\mathcal{R}$ ).

Thus, the dynamics in phase-rotated space as described by  $\check{\mathcal{L}}(\theta)$  is very different from the dynamics described by  $\mathcal{L}$ . Despite having reduced the thermal initial states to single particle states, we have, with  $\check{\mathcal{L}}(\theta)$ , introduced the possibility for the tracer particle to swap positions with a crowder (through  $\mathcal{R}$ ), and to create and annihilate crowder particles in the neighborhood of the tracer particle (through the operators  $\mathcal{C}^\dagger$  and  $\mathcal{C}$ ).

### 2.5. Expansion in terms of particle correlation functions

In this subsection we present a formally exact expansion of the tracer particle PDF. However, before giving the formal expansion, let us discuss the underlying ‘‘philosophy’’ of the expansion. For a tracer particle surrounded by other particles, at ‘‘zeroth order’’ the most relevant effect will be to determine if the next site to jump to is free or not. This effect is contained in the mean field approximation, as previously described. Our expansion is constructed to give the mean field to lowest order. At the next order, as discussed in the introduction, we may find a situation where the tracer particle attempts to jump consecutively to a site where some crowder particle is present. Including this effect, goes beyond mean field, and is contained to next order in our expansion. Higher order terms in our expansion include more complex effects. Such effects are especially prominent for comparatively slow crowder particles,  $r = r_C/r_T \ll 1$  ( $r \rightarrow 0$  is the percolation limit).

Let us now introduce our formal expansion. To that end we take the Laplace transform with respect to time of  $p_c(\mathbf{r}, t|\mathbf{r}_0)$  in Eq. (20):

$$\tilde{p}_c(\mathbf{r}, s|\mathbf{r}_0) = \langle \{\emptyset\} | \langle T_{\mathbf{r}} | \frac{1}{s - \check{\mathcal{L}}} | T_{\mathbf{r}_0} \rangle | \{\emptyset\} \rangle. \quad (25)$$

We proceed by splitting the phase-rotated Liouvillian according to  $\check{\mathcal{L}} = \check{\mathcal{L}}_0 + \gamma \check{\mathcal{L}}'$ , where  $\check{\mathcal{L}}_0 = r_C \mathcal{U}_C + r_T(1-c)\mathcal{U}_T + r_T c \mathcal{R}$  and  $\check{\mathcal{L}}' = \mathcal{C} + \mathcal{C}^\dagger$  correspond to the conservative part and the non-conservative part with respect to the number of crowder particles, respectively, with  $\gamma = r_T \sqrt{c(1-c)}$ . By repeatedly using the identity:

$$\frac{1}{s - \check{\mathcal{L}}} = \frac{1}{s - \check{\mathcal{L}}_0} + \gamma \frac{1}{s - \check{\mathcal{L}}_0} \check{\mathcal{L}}' \frac{1}{s - \check{\mathcal{L}}}, \quad (26)$$

we can write our formal expansion

$$\tilde{p}_c(\mathbf{r}, s|\mathbf{r}_0) = \sum_{j=0}^{\infty} \gamma^{2j} \tilde{\phi}_j(\mathbf{r}, s|\mathbf{r}_0), \quad (27)$$

where

$$\tilde{\phi}_j(\mathbf{r}, s|\mathbf{r}_0) = \langle \{\emptyset\} | \langle T_{\mathbf{r}} | \frac{1}{s - \check{\mathcal{L}}_0} \left( \check{\mathcal{L}}' \frac{1}{s - \check{\mathcal{L}}_0} \right)^{2j} | T_{\mathbf{r}_0} \rangle | \{\emptyset\} \rangle. \quad (28)$$

The absence of odd powers of  $\gamma$  in the sum in Eq. (27) appears because the  $\check{\mathcal{L}}'$  operator creates or destructs only one crowder particle at each application. As neither the initial nor the final states contain crowder particles, we need an even number of applications of this operator to yield a non-zero contribution. We notice that the expansion parameter,

$$\gamma^2 = r_T^2 c(1-c) \leq r_T^2/4, \quad (29)$$

converges to zero for small ( $c \rightarrow 0$ ) or large ( $c \rightarrow 1$ ) crowder concentrations. However, notice (see Eqs. (21), (27) and (28)) that the quantity  $\tilde{\phi}_j(\mathbf{r}, s|\mathbf{r}_0)$  also (in a non-trivial fashion) depends on  $r$  and  $c$ . Therefore, care is required when studying the  $c \rightarrow 0$  and  $c \rightarrow 1$  limits.

To clarify the underlying physics of each term in Eq. (27) let us consider the first few ones. For  $j = 0$  we have, in the time domain,

$$\phi_0(\mathbf{r}, t|\mathbf{r}_0) = \langle \{\emptyset\} | \langle T_{\mathbf{r}} | e^{t(1-c)r_T \mathcal{U}_T} | T_{\mathbf{r}_0} \rangle | \{\emptyset\} \rangle. \quad (30)$$

This expression is the PDF for diffusion of the tracer particle where the jump rate is renormalized by the concentration of empty sites ( $1-c$ ), compared to the single particle PDF in Eq. (7). This thus corresponds to the mean field approximation discussed in the introduction. The fact that only the tracer particle update operator,  $r_T \mathcal{U}_T$ , enters the expression above, and not the full  $\check{\mathcal{L}}_0$ , follows from the fact that the operators  $\mathcal{U}_C$  and  $\mathcal{R}$  act on crowder particle states and that the phase-rotated initial state does not include crowder particles. Note that the thermodynamic result above is independent of the lattice considered.

Going further to the first order correction ( $j = 1$ ) we have the Laplace domain result

$$\tilde{\phi}_1(\mathbf{r}, s|\mathbf{r}_0) = \langle \{\emptyset\} | \langle T_{\mathbf{r}} | \frac{1}{s - r_T(1-c)\mathcal{U}_T} \mathcal{C} \frac{1}{s - \check{\mathcal{L}}_0} \mathcal{C}^\dagger \frac{1}{s - r_T(1-c)\mathcal{U}_T} | T_{\mathbf{r}_0} \rangle | \{\emptyset\} \rangle. \quad (31)$$

The propagator above corresponds to a process where a tracer particle diffuses with a renormalized jump rate (mean field); at a given time a crowder particle is created followed by the evolution of both particles according to  $\check{\mathcal{L}}_0$ . Thereafter the crowder particle is annihilated, followed by the diffusion of the tracer particle.

Considering higher order terms,  $j \geq 2$  in Eq. (27), we notice that the reduction we made for the operator  $\check{\mathcal{L}}'$  for  $\tilde{\phi}_1$  now is more complicated. For example, for  $j = 2$  we find that  $\tilde{\phi}_2$  can be decomposed into two distinct processes: (i) one involving the consecutive creation of two crowder particles followed by their annihilation, and (ii) another one where a crowder particle is created and then destroyed, followed by the creation and subsequent annihilation of a new crowder. This corresponds to the case where the tracer particle consecutively meets two particles. When evaluating higher order terms (arbitrary  $j$ ) one must make sure that the creation and annihilation operators originating from  $\check{\mathcal{L}}'$  are constrained such that no more crows are annihilated than created. Note that all combinations are embedded into the probability  $\tilde{\phi}_j$ : (i) creating  $j$  crowder particles and then annihilating them, (ii) the process of creation of a crowder directly

Lattice	$n_b$	Vector connecting the nearest neighbors is $\mathbf{b} = \pm a\mathbf{v}$
Linear	2	$\mathbf{v} = 1$
Square	4	$\mathbf{v} = \left\{ \begin{pmatrix} 1 \\ 0 \end{pmatrix}, \begin{pmatrix} 0 \\ 1 \end{pmatrix} \right\}$
Cubic	6	$\mathbf{v} = \left\{ \begin{pmatrix} 1 \\ 0 \\ 0 \end{pmatrix}, \begin{pmatrix} 0 \\ 1 \\ 0 \end{pmatrix}, \begin{pmatrix} 0 \\ 0 \\ 1 \end{pmatrix} \right\}$
B.c.c.	8	$\mathbf{v} = \frac{1}{\sqrt{3}} \left\{ \begin{pmatrix} 1 \\ 1 \\ 1 \end{pmatrix}, \begin{pmatrix} -1 \\ 1 \\ 1 \end{pmatrix}, \begin{pmatrix} 1 \\ -1 \\ 1 \end{pmatrix}, \begin{pmatrix} 1 \\ 1 \\ -1 \end{pmatrix} \right\}$
F.c.c.	12	$\mathbf{v} = \frac{1}{\sqrt{2}} \left\{ \begin{pmatrix} 1 \\ 1 \\ 0 \end{pmatrix}, \begin{pmatrix} -1 \\ 1 \\ 0 \end{pmatrix}, \begin{pmatrix} 1 \\ 0 \\ 1 \end{pmatrix}, \begin{pmatrix} -1 \\ 0 \\ 1 \end{pmatrix}, \begin{pmatrix} 0 \\ 1 \\ 1 \end{pmatrix}, \begin{pmatrix} 0 \\ -1 \\ 1 \end{pmatrix} \right\}$

**Table 1.** List of the nearest neighbor displacement vector,  $\mathbf{b}$ , and the number of nearest neighbours,  $n_b$ , for the different considered lattices, where  $a$  is the distance between nearest neighbours.

followed by its annihilation,  $j$  times, and (iii) all intermediate combinations. The expansion proposed in Eq. (27) is based on the assumption that  $\gamma$  is “small”. In practice, the simulation results in Sec. 4 indicate that the convergence of Eq. (27) may be controlled by  $\gamma/r_C$  (for smaller values of this ratio, the first-order approximation becomes better).

It is worth noticing that if the zeroth and first order terms relate to diffusion of one and two interacting particles, respectively, already the second order, involving the diffusion of three interacting particles, is beyond reach of exact calculation in general. In the related context of diffusion in disordered media, a somewhat similar diagrammatic expansion was studied using renormalization group methods [3].

In the next Sec. 3, we will see that for a regular lattice, analysis of the exact expansion provides good estimates for the tracer particle diffusion coefficient.

### 3. Crowding effects on tracer particle diffusion on regular lattices

In this section we focus on diffusion on regular lattices where the separation to nearest neighbors is homogeneous. These lattices fall into the Bravais lattice category, and have translation invariance. In Table 1 we present the definition of the different neighbor displacements,  $\mathbf{b}$ . In Table 2 other characteristic numbers defining the lattice geometry are provided. Below, we first relate the PDF introduced previously to the tracer particle MSD (Sec. 3.1). We then derive the zeroth order contribution to the diffusion constant in Sec. 3.2, followed by results for the first order contribution (Sec. 3.3).

### 3.1. Mean square displacement on regular lattices

For regular lattices we are now interested in the MSD of a tracer particle. Using the definition of the variance of  $p_c(\mathbf{r}, t|\mathbf{r}_0)$  and the expansion in Eq. (27) we obtain

$$\mathcal{MSD}(t) = \sum_{j=0}^{\infty} \gamma^{2j} A_j(t)t, \quad (32)$$

where

$$A_j(t) = \frac{1}{t} \sum_{\mathbf{n}, \mathbf{n}_0} (\mathbf{r}(t) - \mathbf{r}_0)^2 \phi_j(\mathbf{r}, t|\mathbf{r}_0). \quad (33)$$

Using the definition of the correlation factor, Eq. (1), we have

$$f(t, c, r_C, r_T) = \frac{1}{n_b r_T a^2 (1-c)} \sum_{j=0}^{\infty} \gamma^{2j} A_j(t). \quad (34)$$

To proceed, we introduce the Fourier transform of the position of the tracer particle:

$$|\hat{T}_{\mathbf{q}}\rangle = \sum_{\mathbf{r}} e^{-i\mathbf{q}\cdot\mathbf{r}} |T_{\mathbf{r}}\rangle \quad (35)$$

with inverse

$$|T_{\mathbf{r}}\rangle = \frac{1}{(2\pi)^d} \int d^d q e^{i\mathbf{q}\cdot\mathbf{r}} |\hat{T}_{\mathbf{q}}\rangle, \quad (36)$$

where  $\int d^d q = (l_1 \cdots l_d) \int_{-\pi/l_1}^{\pi/l_1} dq_1 \cdots \int_{-\pi/l_d}^{\pi/l_d} dq_d$  with  $l_i = av_i$  ( $i = 1, \dots, d$ ) and  $v_i$  the  $i$ th component of neighboring vector  $\mathbf{v}$  as given in Table 1. The Fourier transform in space associated with  $p_c(\mathbf{r}, t|\mathbf{r}_0)$  is

$$S(\mathbf{q}, t) = \frac{1}{N} \sum_{\mathbf{r}, \mathbf{r}_0} e^{-i\mathbf{q}\cdot(\mathbf{r}-\mathbf{r}_0)} \langle \{\emptyset\} | \langle T_{\mathbf{r}} | e^{t\tilde{\mathcal{L}}} | T_{\mathbf{r}_0} \rangle | \{\emptyset\} \rangle. \quad (37)$$

Using the expansion in Eq. (27) of  $p_c(\mathbf{r}, t|\mathbf{r}_0)$  we have that

$$S(\mathbf{q}, t) = \sum_{j=0}^{\infty} \gamma^{2j} S_j(\mathbf{q}, t), \quad (38)$$

where

$$S_j(\mathbf{q}, t) = \frac{1}{N} \sum_{\mathbf{r}, \mathbf{r}_0} e^{-i\mathbf{q}\cdot(\mathbf{r}-\mathbf{r}_0)} \tilde{\phi}_j(\mathbf{r}, t|\mathbf{r}_0) \quad (39)$$

are the Fourier transforms related to each  $\tilde{\phi}_j(\mathbf{r}, s|\mathbf{r}_0)$  as defined earlier. The MSD now can be extracted from  $S(\mathbf{q}, t)$  as the second order term in  $\mathbf{q}$ , according to

$$S(\mathbf{q}, t) = 1 - \frac{|\mathbf{q}|^2}{2d} \mathcal{MSD}(t) + O[\mathbf{q}^3] \quad (40)$$

where  $|\mathbf{q}|^2 = q_x^2 + q_y^2 + q_z^2$ . The fact that no cross-terms ( $q_x q_y$  etc) appear above follows from the fact that the dynamics for all lattices considered herein is rotationally symmetric. The contribution to the crowding effect then is contained in

$$\bar{A}_j = \lim_{t \rightarrow \infty} A_j(t) = - \lim_{t \rightarrow \infty} \frac{1}{t} \nabla_{\mathbf{q}}^2 S_j(\mathbf{q}, t) \Big|_{\mathbf{0}}, \quad (41)$$

with  $S_j(\mathbf{q}, t)$  given by Eqs. (28) and (39).

### 3.2. Zeroth order: mean field approximation

The zeroth order term in the expansion in the previous subsection is straightforward to derive, because no crowder particle states are involved. The Laplace transform is (see Eqs. (30) and (39))

$$\begin{aligned}\tilde{S}_0(\mathbf{q}, s) &= \frac{1}{N} \sum_{\mathbf{r}, \mathbf{r}_0} e^{-i\mathbf{q} \cdot (\mathbf{r} - \mathbf{r}_0)} \langle \{\emptyset\} | \langle T_{\mathbf{r}} | \frac{1}{s - r_T(1-c)\mathcal{U}_T} | T_{\mathbf{r}_0} \rangle | \{\emptyset\} \rangle \\ &= \frac{1}{s - r_T(1-c) \sum_{\mathbf{b}} (e^{i\mathbf{q} \cdot \mathbf{b}} - 1)},\end{aligned}\quad (42)$$

with  $\sum_{\mathbf{b}}$  the sum over all the neighbor displacements of the considered lattice. We have that  $\sum_{\mathbf{b}} (e^{i\mathbf{q} \cdot \mathbf{b}} - 1) \approx -a^2 \sum_{\mathbf{v}} (\mathbf{q} \cdot \mathbf{v})^2 = -n_b a^2 |\mathbf{q}|^2 / (2d)$ , where in the last step we used the explicit expressions for  $\mathbf{v}$  in Table 1. We thus obtain

$$A_0(t) = A_0 = a^2 n_b r_T (1-c), \quad (43)$$

where  $n_b$  is the number of nearest neighbors. Thus, the lowest order term in our expansion is indeed the mean field result, where the crowded environment provides a renormalization of the diffusion constant for the tracer particle by a factor  $(1-c)$ . As stated previously, the mean field result is a useful approximation as long as  $\gamma^2 = r_T^2 c(1-c)$  is “small”.

Let us now venture beyond the mean field approximation, into the first order of the expansion.

### 3.3. First order: including two-body correlation effects

Consider now the first order term,  $p_1(\mathbf{r}, t | \mathbf{r}_0)$ , as given in Eqs. (31) and (39). We have for the Laplace-Fourier transform that

$$\tilde{S}_1(\mathbf{q}, s) = [\tilde{S}_0(\mathbf{q}, s)]^2 \frac{1}{N} \sum_{\mathbf{r}, \mathbf{r}_0} e^{-i\mathbf{q} \cdot (\mathbf{r} - \mathbf{r}_0)} \langle \{\emptyset\} | \langle T_{\mathbf{r}} | \mathcal{C} \frac{1}{s - \tilde{\mathcal{L}}_0} \mathcal{C}^\dagger | T_{\mathbf{r}_0} \rangle | \{\emptyset\} \rangle. \quad (44)$$

As shown above, we have that  $\tilde{S}_0^2(\mathbf{q}, s) \sim 1/s^2 + \mathcal{O}[\mathbf{q}^2]$  leading to

$$A_1(t)t = L^{-1} \left\{ \frac{1}{s^2} \frac{-4n_b a^2 V(s)}{1 - 2(r_T(1-c) + r_C)V(s)} \right\}, \quad (45)$$

as derived in [Appendix C](#).  $V(s)$  depends on the lattice and is defined respectively for the hypercubic (linear, square and cubic), b.c.c. and f.c.c. lattices according to:

$$V_{\text{hyp}}(s) = \int_{-\pi}^{\pi} \frac{dp_x}{2\pi} \int_{-\pi}^{\pi} \frac{dp_y}{2\pi} \int_{-\pi}^{\pi} \frac{dp_z}{2\pi} \frac{\sin^2(p_x)}{s - 2(r_T(1-c) + r_C) \sum_{\mathbf{v}} (\cos(\mathbf{p} \cdot \mathbf{v}) - 1)} \quad (46)$$

$$V_{\text{bcc}}(s) = 4 \int_{-\pi}^{\pi} \frac{dp_x}{2\pi} \int_{-\pi}^{\pi} \frac{dp_y}{2\pi} \int_{-\pi}^{\pi} \frac{dp_z}{2\pi} \frac{\sin^2(p_x/\sqrt{3}) \cos^2(p_y/\sqrt{3}) \cos^2(p_z/\sqrt{3})}{s - 2(r_T(1-c) + r_C) \sum_{\mathbf{v}} (\cos(\mathbf{p} \cdot \mathbf{v}) - 1)} \quad (47)$$

$$V_{\text{fcc}}(s) = 2 \int_{-\pi}^{\pi} \frac{dp_x}{2\pi} \int_{-\pi}^{\pi} \frac{dp_y}{2\pi} \int_{-\pi}^{\pi} \frac{dp_z}{2\pi} \frac{\sin^2(p_x/\sqrt{2}) \cos(p_y/\sqrt{2}) (\cos(p_y/\sqrt{2}) + \cos(p_z/\sqrt{2}))}{s - 2(r_T(1-c) + r_C) \sum_{\mathbf{v}} (\cos(\mathbf{p} \cdot \mathbf{v}) - 1)} \quad (48)$$

with  $r = r_C/r_T$  is the relative crowder particle jump rate and where the unit vectors  $\mathbf{v}$  are listed in Table 1 for the different lattice types considered. For linear and square lattices the integrals in  $V_{\text{hyp}}(s)$  are replaced by integrals over  $p_x$  and over  $(p_x, p_y)$ , respectively. Similar results were derived for translationally non-invariant lattices, such as honeycomb and diamond, in Ref. [26]. There, also some details were given regarding the derivation for linear, square and cubic lattices. For these, the results given above match those of Nakazato and Kitahara [15]. The derivation provided here extends the Nakazato and Kitahara results to f.c.c. and b.c.c. lattices.

Taking into account only the zeroth and first order of the expansion (34) we find the first order approximation of the correlation factor

$$f_{\text{first-order}}(t) = 1 + \gamma^2 \frac{A_1(t)}{A_0} \quad (49)$$

$$= 1 - \frac{1}{t} L^{-1} \left\{ \frac{1}{s^2} \frac{4r_T c V(s)}{1 - 2(r_T(1 - 3c) + r_C)V(s)} \right\}. \quad (50)$$

where we used the mean field result in Eq. (43), and  $A_1(t)$  is given in Eq. (45). The results above generalize the Nakazato and Kitahara results [15] to a larger class of lattices.

We will later show by simulations (Sec. 4) that the first-order approximation given above overestimates the true correlation factor for the cases considered. This finding is consistent with (but does not prove) that higher order terms in the expression (34) (second order and beyond) linked to high order correlation effect, contribute negatively to the diffusion, i.e., that  $A_j(t) < 0$  also for  $j \geq 2$ .

For a one dimensional lattice the coefficient  $V(s)$ , Eq. (46), can be estimated yielding a correlation factor (see Appendix D)

$$f_{\text{first-order}}(t) \underset{t \rightarrow \infty}{=} \frac{1}{c} \sqrt{\frac{r+1-c}{\pi r_T t}}. \quad (51)$$

where  $r = r_C/r_T$ . Existing exact results are  $f(t \rightarrow \infty) = \frac{1}{c} \sqrt{r_{\text{eff}}/(r_T^2 \pi t)}$  asymptotically [27, 28], where the quantity  $r_{\text{eff}} = (n+1)r_C r_T / (r_C + n r_T)$ . In the thermodynamic limit,  $n \rightarrow \infty$  as considered here, we hence have  $r_{\text{eff}} = r_C$ . We thus notice that for this case indeed  $f(t) < f_{\text{first-order}}(t)$ , and the scaling with time agrees with exact results, i.e.,  $\text{MSD}(t) \underset{t \rightarrow \infty}{\sim} t^{1/2}$ .

For higher dimensions we are restricted to the long time limit which becomes (see Appendix D):

$$f_{\text{first-order}}(\infty) = 1 - \frac{2c}{2c + (r+1-c)\beta}, \quad (52)$$

with  $(\beta+1)^{-1} = 2r_T(r+1-c)V(0)$ , where  $\beta$  is a structure factor depending on the lattice geometry, and  $r = r_C/r_T$  is the relative crowder particle jump rate as before. The values of the structure factors are listed in Table 2 for the considered lattices, together with other typical characteristics (dimension and nearest neighbor count). For the one-dimensional (linear) lattice we have  $\beta = 0$ , giving  $f_{\text{first-order}}(\infty) = 0$ , indicating the

Lattice	$d$	$n_b$	$\beta$
Linear	1	2	0
Square	2	4	$2/(\pi - 2)$
Cubic	3	6	3.7655
B.c.c.	3	8	5.04863
F.c.c.	3	12	8.24308

**Table 2.** Table of lattice characteristics, where  $d$  is the dimension of the lattice,  $n$  the nearest neighbor count, and  $\beta$  a structural factor appearing in the correlation factor, Eq. (52).

sub-linear scaling of the MSD with time as discussed previously. For the other lattices we have  $f_{\text{first-order}}(\infty) \neq 0$ , representing linear scaling of the MSD. In the next section, we compare the first-order approximation above to simulation results.

#### 4. Comparison with simulation results

In this section we will present a comparison between the approximations given previously and numerical simulations. We first describe the Gillespie algorithm used to simulate the problem. We then present and comment on our simulation results, and their difference and similarity to the approximate results derived in the previous section.

##### 4.1. Simulations using the Gillespie algorithm

We describe here, in pseudocode, the algorithm used to simulate a many-particle system. Steps (iii) to (vi) is a description of the *trial-and-error-method*, outlined in Ref. [29] (except that we here use a fixed time step between attempted jumps, see Step (v) below).

- (i) We start by assigning jump rates for each of the  $n_b$  directions and  $n$  crowding particles, and construct a partial sum over them, such that:

$$p_0 = 0, \quad p_a = \sum_{i=1}^a r_i, \quad a = 1, \dots, n_b \cdot n; \quad r_i = \begin{cases} r_T, & i \leq n_b. \\ r_C, & i > n_b \end{cases} \quad (53)$$

where  $r_T$  and  $r_C$  correspond to the jump rate of the tracer and crowder particle, respectively.

- (ii) Place the tracer particle at the center of the lattice, and place the remaining particles randomly on the lattice, by using the Bebbington algorithm:

Cycle through all lattice sites (except the position of the tracer particle), and place a particle at the current site with the probability  $a/m$ , where  $a \in [0, n]$  is the number of particles left to place, and  $m \in [0, N - 1]$  is the number of lattice sites left to cycle through [30].

Set the time equal to zero.



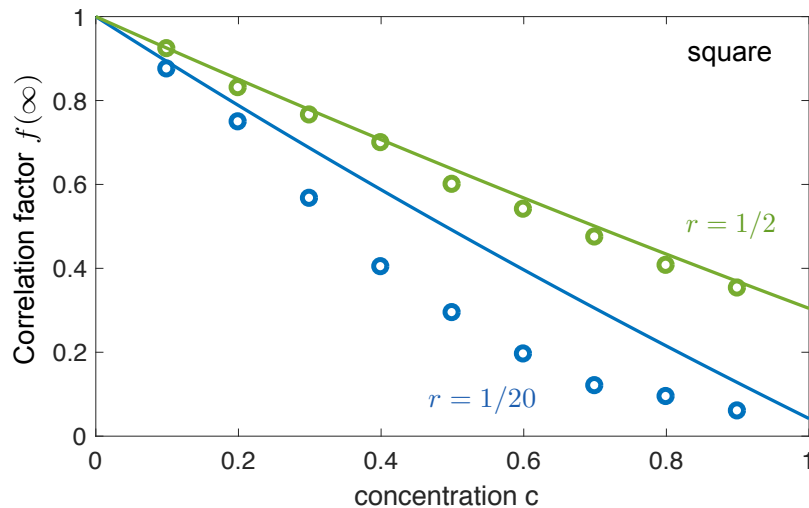


**Figure 3.** Simulations and theoretical estimation for the correlation factor in the long time limit for two-dimensional square lattice: The correlation factor,  $f$ , is shown as a function of the concentration  $c$  for a relative jump rate  $r = 1/20$  in blue (lower curves) and  $r = 1/2$  in green (upper curves). The marks correspond to the Gillespie simulations ( $M = 400$  for  $r = 1/20$  and  $M = 1000$  for  $r = 1/2$ ), while the full curves are determined by the first order approximation given in Eq. (52).

- (iii) Draw a random number  $0 < r < 1$  with uniform distribution, and find the element with label  $k$  such that

$$p_k \leq r p_{n_b n} < p_{k+1}. \quad (54)$$

- (iv) Convert  $k$  to the corresponding particle and direction, and move it, provided the chosen site is unoccupied.
- (v) Update the time to  $t \rightarrow t + \frac{1}{p_{n_b n}}$ .
- (vi) Return to step (iii) until  $t \geq t_{\max}$ .
- (vii) Return to step (ii) to start the simulation of the next trajectory.

As a stop time, we choose  $t_{\max} = 10t_{\min}$  in all simulations, where  $t_{\min}$  is given in Eq. (E.2). The number of trajectories is denoted by  $M$ .

Our simulation software package (written in C++) is available from <https://github.com/impaktor/diffusion> and is released under the GNU General Public License (GPL) [31].

Based on the tracer particle trajectories, diffusion constants were obtained using weighted least-squares fitting to the MSD, see Appendix E for details.

#### 4.2. Comparison between simulations and analytic predictions

For a set of two- and three-dimensional lattices, the correlation factor is shown in Fig. 3 and Fig. 4, together with the corresponding first-order approximation  $f_{\text{first-order}}$ , Eq. (52). We consider only long-time results for the correlation factor, and study its

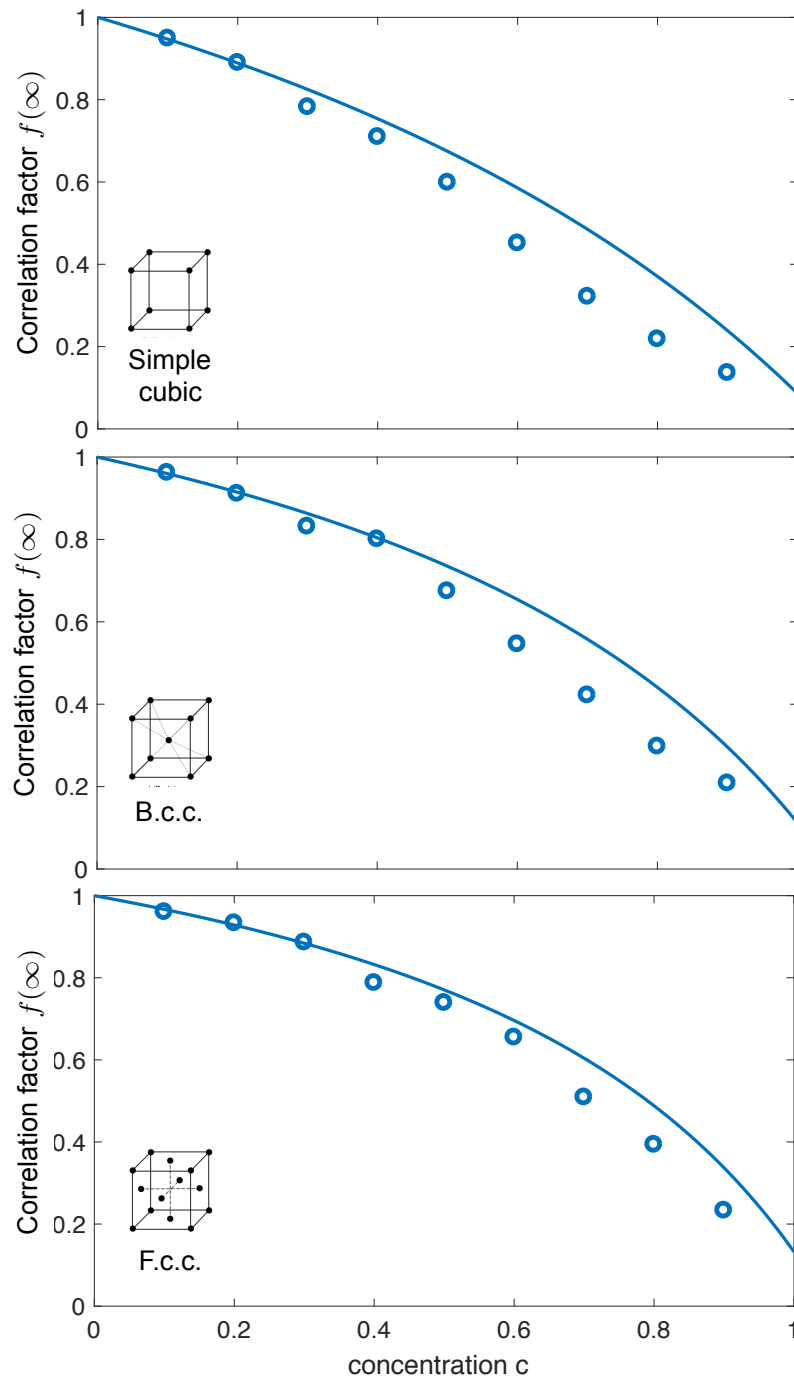


**Figure 4.** Simulations and theoretical predictions for the correlation factor in the long-time limit for three-dimensional lattices. Shown is the correlation factor  $f$  as a function of the concentration  $c$  for a relative jump rate  $r = 1/20$ . The lattice geometry is indicated in inset (simple cubic, b.c.c. and f.c.c. lattices). The marks correspond to the Gillespie simulations ( $M = 300$  trajectories), while the full curves are determined by the first-order approximation given in Eq. (52).

concentration dependence. For the two-dimensional square lattice we consider two jump rates,  $r = 1/20$  and  $r = 1/2$ . The lattice size is  $400 \times 400$  sites with periodic boundary conditions, and the results are averaged over 400 trajectories for  $r = 1/20$  and 1000 trajectories for  $r = 1/2$  (Fig. 3). For the three-dimensional lattice we set the relative jump rates to  $r = 1/20$ . Here, we choose a lattice size of  $200 \times 200 \times 200$  with periodic boundary conditions, and the results are averaged over an ensemble of 300 trajectories (Fig. 4).

For all of the lattices considered, we see that the simulation results are below the first-order approximation  $f_{\text{first-order}}$ . Thus, the first-order result Eq. (27) appears to set an upper bound for the correlation factor. This finding will be useful in future attempts to calculate exact, or approximate, expressions for the higher order terms in Eq. (34). In Fig. 3 we see that upon decreasing  $r$  the discrepancy between the simulation and Eq. (52) increases. This indicates non-negligible contributions of higher orders of the expansion Eq. (27) for slowly diffusing tracer particles. However, we see that  $f_{\text{first-order}}$ , in general, still gives a very good estimate of the correlation factor.

## 5. Summary

To summarize, we have here presented a general derivation of the PDF, and MSD, for the position of a tracer particle diffusing in a crowded system, where the tracer particle has a different diffusion constant from the crowder particles. The general derivation is based on a polaron-like mapping like in Ref. [15]. We showed that the tracer particle PDF can be expressed as an expansion in terms of crowder particle correlation functions. Focusing on regular lattices, we then showed that the first order of the expansion can be evaluated for regular lattices extending the results of Nakazato and Kitahara [15]. We provide extensive numerical analysis for the different lattices considered, suggesting that  $f_{\text{first-order}}$  overestimates the true correlation factor.

The present work, besides proposing a generic approach to diffusion in a crowded network, improves our understanding of diffusion in crowded regular lattices, especially in a context of slowly diffusive environments. The potential range of application of this result extends from biophysics to solid state physics or other types of dynamics on networks.

## Acknowledgments

This work was supported by the Swedish Research Council (grant no. 2009–2924 and 2014–4305), the Crafoord Foundation (grant 20110588), the John Templeton Foundation (grant ID 43467) and French ANR (grant ACHN - C-FLigHT). SP would like to thank Mauro Paternostro and Gabriele De Chiara for their support. GM would like to thank the Department of Astronomy and Theoretical Physics, Lund University, for hospitality.

## Appendix A. Phase rotation of the initial states

In this appendix we, for completeness, provide a derivation of the result given in Ref. [15] for the phase-rotated initial states.

Consider Eq. (11), which we rewrite according to:

$$\begin{aligned} G(\mathbf{r}, t | \mathbf{r}_0; x) &= \langle \{\emptyset\} | \langle T_{\mathbf{r}} | W^-(x) e^{-\theta S} e^{t\mathcal{L}} e^{+\theta S} W^+(x) | T_{\mathbf{r}_0} \rangle | \{\emptyset\} \rangle \\ &= \langle T_{\mathbf{r}} | \langle \{\emptyset\} | W^-(x) e^{t\check{\mathcal{L}}(\theta)} W^+(x) | T_{\mathbf{r}_0} \rangle | \{\emptyset\} \rangle, \end{aligned} \quad (\text{A.1})$$

where  $|T_{\mathbf{r}_0}\rangle|\{\emptyset\}\rangle$  denotes the state of no occupancy at all sites except at the tracer particle position  $\mathbf{r}_0$  as before. Also,

$$W^+(x) = e^{-\theta S} \prod_{j=1}^N (1 + \sqrt{x} |C_{\mathbf{u}_j}\rangle \langle 0_{\mathbf{u}_j}|), \quad (\text{A.2})$$

$$W^-(x) = \prod_{j=1}^N (1 + \sqrt{x} |0_{\mathbf{u}_j}\rangle \langle C_{\mathbf{u}_j}|) e^{+\theta S}, \quad (\text{A.3})$$

and

$$\check{\mathcal{L}}(\theta) = e^{-\theta S} \mathcal{L} e^{+\theta S}. \quad (\text{A.4})$$

In the last step in Eq. (A.1) we used the following result

$$\begin{aligned} e^{-\theta S} e^{t\mathcal{L}} e^{+\theta S} &= e^{-\theta S} [1 + \mathcal{L}t + \frac{1}{2!} (\mathcal{L}t)^2 + \dots] e^{+\theta S} \\ &= 1 + t e^{-\theta S} \mathcal{L} e^{+\theta S} + \frac{t^2}{2!} e^{-\theta S} \mathcal{L} \mathcal{L} e^{+\theta S} + \dots \\ &= 1 + t e^{-\theta S} \mathcal{L} e^{+\theta S} + \frac{t^2}{2!} e^{-\theta S} \mathcal{L} e^{+\theta S} e^{-\theta S} \mathcal{L} e^{+\theta S} + \dots \\ &= \exp[t e^{-\theta S} \mathcal{L} e^{+\theta S}] = \exp[t \check{\mathcal{L}}(\theta)], \end{aligned} \quad (\text{A.5})$$

where  $S$  should not depend on the location of the tracer particle site. Following Nakazato and Kitahara [15] one chooses

$$S = \sum_{j=1}^N S_j, \quad (\text{A.6})$$

where  $S_j = |C_{\mathbf{u}_j}\rangle \langle 0_{\mathbf{u}_j}| - |0_{\mathbf{u}_j}\rangle \langle C_{\mathbf{u}_j}|$ . Now,

$$e^{-\theta S_j} = 1 - \theta S_j + \frac{\theta^2}{2!} S_j^2 - \frac{\theta^3}{3!} S_j^3 + \frac{\theta^4}{4!} S_j^4 + \dots \quad (\text{A.7})$$

We have

$$\begin{aligned} S_j^2 &= (|C_{\mathbf{u}_j}\rangle \langle 0_{\mathbf{u}_j}| - |0_{\mathbf{u}_j}\rangle \langle C_{\mathbf{u}_j}|) (|C_{\mathbf{u}_j}\rangle \langle 0_{\mathbf{u}_j}| - |0_{\mathbf{u}_j}\rangle \langle C_{\mathbf{u}_j}|) \\ &= -|C_{\mathbf{u}_j}\rangle \langle C_{\mathbf{u}_j}| - |0_{\mathbf{u}_j}\rangle \langle 0_{\mathbf{u}_j}| = -I_j, \end{aligned} \quad (\text{A.8})$$

where  $I_j = |C_{\mathbf{u}_j}\rangle\langle C_{\mathbf{u}_j}| + |0_{\mathbf{u}_j}\rangle\langle 0_{\mathbf{u}_j}|$  is an identity operator which leaves any no-tracer state unchanged. Therefore

$$\begin{aligned} S_j^3 &= -S_j, \\ S_j^4 &= (-I_j)(-I_j) = I_j, \end{aligned} \quad (\text{A.9})$$

etc. Eq. (A.7) now becomes

$$\begin{aligned} e^{-\theta S_j} &= I_j - \theta S_j - \frac{\theta^2}{2!} I_j - \frac{\theta^3}{3!} S_j - \frac{\theta^4}{4!} I_j + \dots \\ &= \cos \theta I_j - \sin \theta S_j. \end{aligned} \quad (\text{A.10})$$

We now have

$$\begin{aligned} e^{-\theta S_j} (1 + \sqrt{x} |C_{\mathbf{u}_j}\rangle\langle 0_{\mathbf{u}_j}|) |T_{\mathbf{r}_0}\rangle |\{\emptyset\}\rangle &= [\cos \theta I_{\mathbf{u}_j} - \sin \theta (|C_{\mathbf{u}_j}\rangle\langle 0_{\mathbf{u}_j}| - |0_{\mathbf{u}_j}\rangle\langle C_{\mathbf{u}_j}|)] \\ &\quad \times (1 + \sqrt{x} |C_{\mathbf{u}_j}\rangle\langle 0_{\mathbf{u}_j}|) |T_{\mathbf{r}_0}\rangle |\{\emptyset\}\rangle \\ &= [(\cos \theta + \sin \theta \sqrt{x}) \\ &\quad + (\cos \theta \sqrt{x} - \sin \theta) (|C_{\mathbf{u}_j}\rangle\langle 0_{\mathbf{u}_j}|) |T_{\mathbf{r}_0}\rangle |\{\emptyset\}\rangle], \end{aligned} \quad (\text{A.11})$$

where we used the fact that  $|0_{\mathbf{u}_j}\rangle\langle C_{\mathbf{u}_j}| |T_{\mathbf{r}_0}\rangle |\{\emptyset\}\rangle = 0$ . If we now choose  $\theta$  such that  $\cos \theta \sqrt{x} = \sin \theta$ , i.e.,  $\tan \theta = \sqrt{x}$ , so that  $\sin \theta = \sqrt{x}/\sqrt{1+x}$  and  $\cos \theta = 1/\sqrt{1+x}$ , then

$$\begin{aligned} W^+(\theta, x) |T_{\mathbf{r}_0}\rangle |\{\emptyset\}\rangle &= \prod_{l=1}^N (\cos \theta + \sin \theta \sqrt{x}) |T_{\mathbf{r}_0}\rangle |\{\emptyset\}\rangle \\ &= (1+x)^{(N-1)/2} |T_{\mathbf{r}_0}\rangle |\{\emptyset\}\rangle. \end{aligned} \quad (\text{A.12})$$

Similarly, one finds,

$$\langle \{\emptyset\} | \langle T_{\mathbf{r}} | W^-(x) = \langle \{\emptyset\} | \langle T_{\mathbf{r}} | (1+x)^{(N-1)/2}. \quad (\text{A.13})$$

Therefore, Eq. (A.1) becomes:

$$G(\mathbf{r}, t | \mathbf{r}_0; x) = (1+x)^{(N-1)} \langle \{\emptyset\} | \langle T_{\mathbf{r}} | e^{t\check{\mathcal{L}}(\theta)} |T_{\mathbf{r}_0}\rangle |\{\emptyset\}\rangle, \quad (\text{A.14})$$

which, when combined with Eq. (10), leads to Eq. (13) in the main text.

## Appendix B. Phase-rotated Liouvillian

Consider the phase-rotated Liouvillian given in Eq. (13). Application of The Baker-Campbell-Hausdorff formula [32] to this expression gives

$$\check{\mathcal{L}} = e^{-\theta S} \mathcal{L} e^{+\theta S} = \mathcal{L} - \theta [S, \mathcal{L}] + \frac{\theta^2}{2!} [S, [S, \mathcal{L}]] - \frac{\theta^3}{3!} [S, [S, [S, \mathcal{L}]]] + \dots, \quad (\text{B.1})$$

where  $\mathcal{L} = r_T \mathcal{U}_T + r_C \mathcal{U}_C$  is defined through Eq. (6) and  $S$  is given in Eq. (A.6). Consider now the second term on the right-hand side of Eq. (B.1). After some algebra, one finds

$$[S, \mathcal{L}] = -r_T \mathcal{T}, \quad (\text{B.2})$$

where  $\mathcal{T} = \mathcal{C} + \mathcal{C}^\dagger$ , and where  $\mathcal{C}$  and  $\mathcal{C}^\dagger$  are given in Eqs. (23), and (24) in the main text, respectively. Proceeding to higher orders, we find after some lengthier algebra, that

$$[S, [S, \mathcal{L}]] = -2r_T \mathcal{U}_T + 2r_T \mathcal{R}, \quad (\text{B.3})$$

where  $\mathcal{R}$  is given by Eq. (22) in the main text. The next order term becomes:

$$[S, [S, [S, \mathcal{L}]]] = 4r_T \mathcal{T}. \quad (\text{B.4})$$

Proceeding in this manner, one then gets

$$\begin{aligned} \check{\mathcal{L}} &= r_C \mathcal{U}_C + r_T \left( \mathcal{U}_T + \theta \mathcal{T} + \frac{\theta^2}{2!} 2[-\mathcal{U}_T + \mathcal{R}] - \frac{\theta^3}{3!} [4\mathcal{T}] \right. \\ &\quad \left. - \frac{\theta^4}{4!} 8[-\mathcal{U}_T + \mathcal{R}] + \frac{\theta^5}{5!} [16\mathcal{T}] + \dots \right) \\ &= r_C \mathcal{U}_C + r_T \left( \mathcal{U}_T + \frac{1}{2} \left[ -\frac{(2\theta)^2}{2!} + \frac{(2\theta)^4}{4!} + \dots \right] [\mathcal{U}_T - \mathcal{R}] \right. \\ &\quad \left. + \frac{\mathcal{T}}{2} \left[ (2\theta) - \frac{(2\theta)^3}{3!} + \frac{(2\theta)^5}{5!} - \dots \right] \right) \\ &= r_C \mathcal{U}_C + r_T \left( \mathcal{U}_T + \frac{\cos 2\theta - 1}{2} [\mathcal{U}_T - \mathcal{R}] \right) + r_T \frac{\sin 2\theta}{2} \mathcal{T} \\ &= r_C \mathcal{U}_C + r_T \left( \frac{1 + \cos 2\theta}{2} \mathcal{U}_T + \frac{1 - \cos 2\theta}{2} \mathcal{R} + \frac{\sin 2\theta}{2} \mathcal{T} \right) \\ &= r \mathcal{U}_C + r_T \cos^2 \theta \mathcal{U}_T + r_T \sin^2 \theta \mathcal{R} + r_T \sin \theta \cos \theta \mathcal{T}. \end{aligned} \quad (\text{B.5})$$

which is the result given in the main text, Eq. (21).

### Appendix C. Two-body correlation function

In this appendix we derive an explicit expression for  $\tilde{S}_1(\mathbf{q}, s)$ , see Eq. (44), which quantifies two-body correlation effects in the phase-rotated domain. The derivation is similar to Ref. [26] where related quantities are derived for honeycomb and diamond lattices.

In order to take into account two-body correlations we need to explicitly determine Eq. (44), which we write:

$$\begin{aligned} \tilde{S}_1(\mathbf{q}, s) &= [\tilde{S}_0(\mathbf{q}, s)]^2 \frac{1}{N} \sum_{\mathbf{r}, \mathbf{r}_0} e^{-i\mathbf{q} \cdot (\mathbf{r} - \mathbf{r}_0)} \\ &\quad \times \sum_{\mathbf{b}, \mathbf{b}'} [\tilde{Q}(\mathbf{r}, \mathbf{b}; s | \mathbf{r}_0, \mathbf{b}') - \tilde{Q}(\mathbf{r} + \mathbf{b}, -\mathbf{b}; s | \mathbf{r}_0, \mathbf{b}') \\ &\quad - \tilde{Q}(\mathbf{r}, \mathbf{b}; s | \mathbf{r}_0 - \mathbf{b}', \mathbf{b}') + \tilde{Q}(\mathbf{r} + \mathbf{b}, -\mathbf{b}; s | \mathbf{r}_0 - \mathbf{b}', \mathbf{b}')], \end{aligned} \quad (\text{C.1})$$

where we introduced

$$Q(\mathbf{r}, \mathbf{\Delta}; t | \mathbf{r}_0, \mathbf{\Delta}_0) = \langle \{\emptyset\} | \langle T_{\mathbf{r}} | \langle C_{\mathbf{r}+\mathbf{\Delta}} | e^{t\tilde{\mathcal{L}}_0} | T_{\mathbf{r}_0} \rangle | C_{\mathbf{r}_0+\mathbf{\Delta}_0} \rangle | \{\emptyset\} \rangle, \quad (\text{C.2})$$

which is the probability that the tracer particle is at position  $\mathbf{r}$  with the crowder particle at a separation  $\mathbf{\Delta}$  at time  $t$ . The initial tracer particle position is  $\mathbf{r}_0$  and the initial separation vector is  $\mathbf{\Delta}_0$ . We will below derive an explicit master equation for  $Q(\mathbf{r}, \mathbf{\Delta}; t | \mathbf{r}_0, \mathbf{\Delta}_0)$ . Fourier transforming  $(\hat{\bullet})$  Eq. (C.2) with respect to the tracer position from its initial position,  $\mathbf{r} - \mathbf{r}_0$ , and Laplace transforming  $(\tilde{\bullet})$  with respect to time  $t$ , we have

$$\tilde{Q}(\mathbf{q}, \mathbf{\Delta}, s | \mathbf{\Delta}_0) = \int_0^\infty dt e^{-st} \frac{1}{N} \sum_{\mathbf{r}, \mathbf{r}_0} e^{-i\mathbf{q} \cdot (\mathbf{r} - \mathbf{r}_0)} Q(\mathbf{r}, \mathbf{\Delta}; t | \mathbf{r}_0, \mathbf{\Delta}_0). \quad (\text{C.3})$$

Eq. (C.1) can now be written as

$$\tilde{S}_1(\mathbf{q}, s) = \frac{1}{N} [\tilde{S}_0(\mathbf{q}, s)]^2 \sum_{\mathbf{b}, \mathbf{b}'} (1 - e^{i\mathbf{q} \cdot \mathbf{b}'}) \left[ \tilde{Q}(\mathbf{q}, \mathbf{b}, s | \mathbf{b}') - e^{i\mathbf{q} \cdot \mathbf{b}} \tilde{Q}(\mathbf{q}, -\mathbf{b}, s | \mathbf{b}') \right]. \quad (\text{C.4})$$

To first order in  $\gamma^2$ , the structure factor is now

$$\tilde{S}_1(\mathbf{q}, s) \approx \tilde{S}_0(\mathbf{q}, s) + \gamma^2 \tilde{S}_1(\mathbf{q}, s) + \mathcal{O}[\gamma^4]. \quad (\text{C.5})$$

The contribution to the MSD of  $\tilde{S}_1(\mathbf{q}, s)$  is connected to the second order term in the expansion of  $\tilde{S}(\mathbf{q}, s)$  in  $\mathbf{q}$  (c.f. Eq. (41)). For all lattices considered here, we have that if  $\mathbf{b}$  is a nearest neighbour, then  $-\mathbf{b}$  is also a nearest neighbour vector. Using this fact, and that  $\tilde{S}_0(\mathbf{q}, s) \sim 1/s + \mathcal{O}[\mathbf{q}^2]$  the second order expansion of  $S_1$  becomes

$$\tilde{S}_1(\mathbf{q}, s) = \frac{1}{s^2} G(s) + \mathcal{O}[\mathbf{q}^4] \quad (\text{C.6})$$

with

$$G(s) = \sum_{\mathbf{b}, \mathbf{b}'} (\mathbf{q} \cdot \mathbf{b})(\mathbf{q} \cdot \mathbf{b}') \tilde{Q}(\mathbf{0}, \mathbf{b}, s | \mathbf{b}'). \quad (\text{C.7})$$

Thus, in order to determine the MSD we need to know determine the  $\mathbf{q} \rightarrow 0$  limit of the quantity  $\tilde{Q}(\mathbf{q}, \mathbf{\Delta}, s | \mathbf{\Delta}_0)$ .

Consider now the definition Eq. (C.2), and let us derive a master equation for  $Q(\mathbf{r}, \mathbf{\Delta}; t | \mathbf{r}_0, \mathbf{\Delta}_0)$ . To that end, we take the derivative with respect to time and use the operator identity  $\partial_t \exp[t\tilde{\mathcal{L}}] = \tilde{\mathcal{L}} \exp[t\tilde{\mathcal{L}}]$ . By further using the orthogonality relation, Eq. (4), we arrive at

$$\begin{aligned} \partial_t Q(\mathbf{r}, \mathbf{\Delta}; t) &= r_T c \sum_{\mathbf{b}} \delta_{\mathbf{\Delta}, \mathbf{b}} (Q(\mathbf{r} + \mathbf{\Delta}, -\mathbf{\Delta}; t) - Q(\mathbf{r}, \mathbf{\Delta}; t)) + \sum_{\mathbf{b}} (1 - \delta_{\mathbf{\Delta}, \mathbf{0}} - \delta_{\mathbf{\Delta}, \mathbf{b}}) \\ &\times \left[ r_T (1 - c) (Q(\mathbf{r} + \mathbf{b}, \mathbf{\Delta} - \mathbf{b}; t) - Q(\mathbf{r}, \mathbf{\Delta}; t)) + r_C (Q(\mathbf{r}, \mathbf{\Delta} - \mathbf{b}; t) - Q(\mathbf{r}, \mathbf{\Delta}; t)) \right]. \end{aligned} \quad (\text{C.8})$$

In the derivation above, we left the initial conditions implicit, and used that  $Q(\mathbf{r}, \mathbf{\Delta} = 0; t|\mathbf{r}_0, \mathbf{\Delta}_0) = 0$ , [26] i.e. two particles cannot occupy the same lattice site. The first term on the right hand side above originates from the  $\mathcal{R}$  operator. The  $\delta$ -functions appearing in the remaining terms make sure there cannot be jumps into and out of the “forbidden” state  $\mathbf{\Delta} = 0$ .

To proceed, we take the Laplace and Fourier transforms [see Eq. (C.3)] of Eq. (C.8). We also take the Fourier-transform with respect to  $\mathbf{\Delta}$  (Fourier variable  $\mathbf{p}$ ). By rearranging the terms in the transformed version of Eq. (C.8) and by subsequently performing the inverse Fourier-transform with respect to  $\mathbf{p}$  we arrive at

$$\begin{aligned} \tilde{Q}(\mathbf{q}, \mathbf{\Delta}, s|\mathbf{\Delta}') &= e^{-i\mathbf{q}\cdot\mathbf{r}_0}\omega(\mathbf{q}, \mathbf{\Delta}-\mathbf{\Delta}', s) + \sum_{\mathbf{b}} \left[ r_T c (\omega(\mathbf{q}, \mathbf{\Delta} + \mathbf{b}, s)e^{-i\mathbf{q}\cdot\mathbf{b}} - \omega(\mathbf{q}, \mathbf{\Delta} - \mathbf{b}, s)) \right. \\ &\quad \left. + r_T(1-c) (\omega(\mathbf{q}, \mathbf{\Delta} - \mathbf{b}, s) - \omega(\mathbf{q}, \mathbf{\Delta}, s)e^{-i\mathbf{q}\cdot\mathbf{b}}) + r_C (\omega(\mathbf{q}, \mathbf{\Delta} - \mathbf{b}, s) - \omega(\mathbf{q}, \mathbf{\Delta}, s)) \right] \\ &\quad \times \tilde{Q}(\mathbf{q}, \mathbf{b}, s|\mathbf{\Delta}') \end{aligned} \quad (\text{C.9})$$

with

$$\omega(\mathbf{q}, \mathbf{\Delta}, s) = \frac{1}{(2\pi)^d} \int d^d p \frac{e^{i\mathbf{p}\cdot\mathbf{\Delta}}}{s - r_T(1-c) \sum_{\mathbf{b}} (e^{-i\mathbf{q}\cdot\mathbf{b}} e^{i\mathbf{p}\cdot\mathbf{b}} - 1) - r_C \sum_{\mathbf{b}} (e^{-i\mathbf{p}\cdot\mathbf{b}} - 1)}. \quad (\text{C.10})$$

where  $\int d^d p = (l_1 \cdots l_d) \int_{-\pi/l_1}^{\pi/l_1} dp_1 \cdots \int_{-\pi/l_d}^{\pi/l_d} dp_d$  with  $l_i = av_i$  ( $i = 1, \dots, d$ ) and  $\mathbf{v}$  is given in Table 1. By letting  $\mathbf{q} \rightarrow 0$  in Eq. (C.9), we have an equation for the sought quantity,  $\tilde{Q}(\mathbf{q} = 0, \mathbf{b}, s|\mathbf{b}')$ , see Eq. (C.7). More precisely, by letting  $\mathbf{q} \rightarrow 0$  and by setting  $\mathbf{\Delta}' = \mathbf{b}'$  and  $\mathbf{\Delta} = \mathbf{b}''$  in Eq. (C.9) for all nearest neighbour vectors  $\mathbf{b}''$ , we get (for each  $\mathbf{b}'$ ) a linear system of equations. The size of this system of equations is equal to the number of nearest neighbours for each lattice, in general.

For all lattices considered herein, we are fortunate that one need not solve explicitly the full set of systems of equations provided by Eq. (C.9). Instead, one will get a scalar equation for the quantity  $G(s)$ , see Eq. (C.7), directly. To show this, we let  $\mathbf{q} \rightarrow 0$  in Eq. (C.9) and set  $\mathbf{\Delta} = \mathbf{b}$  and  $\mathbf{\Delta}' = \mathbf{b}'$ . By subsequently multiplying Eq. (C.9) by  $(\mathbf{q} \cdot \mathbf{b})(\mathbf{q} \cdot \mathbf{b}')$  and summing over  $\mathbf{b}$  and  $\mathbf{b}'$  we find that

$$\begin{aligned} G(s) &= \sum_{\mathbf{b}, \mathbf{b}'} (\mathbf{q} \cdot \mathbf{b})(\mathbf{q} \cdot \mathbf{b}') R(\mathbf{b}, \mathbf{b}', s) \\ &\quad + (-2r_T c + [r_T(1-c) + r_C]) \sum_{\mathbf{b}, \mathbf{b}', \mathbf{b}''} (\mathbf{q} \cdot \mathbf{b})(\mathbf{q} \cdot \mathbf{b}'') R(\mathbf{b}, \mathbf{b}'', s) \tilde{Q}(\mathbf{0}, \mathbf{b}, s|\mathbf{b}'), \end{aligned} \quad (\text{C.11})$$

where

$$R(\mathbf{b}, \mathbf{b}', s) = \frac{1}{(2\pi)^d} \int d^d p \frac{\sin(\mathbf{p} \cdot \mathbf{b}) \sin(\mathbf{p} \cdot \mathbf{b}')}{s - [r_T(1-c) + r_C] \sum_{\tilde{\mathbf{b}}} (e^{i\mathbf{p}\cdot\tilde{\mathbf{b}}} - 1)}. \quad (\text{C.12})$$

In the derivation leading up to (C.11) we used the facts that

$$\frac{1}{(2\pi)^d} \int d^d p \frac{\sin(\mathbf{p} \cdot \mathbf{b}) \cos(\mathbf{p} \cdot \mathbf{b}')}{s - [r_T(1-c) + r_C] \sum_{\tilde{\mathbf{b}}} (e^{i\mathbf{p}\cdot\tilde{\mathbf{b}}} - 1)} = 0 \quad (\text{C.13})$$



and that

$$\frac{1}{(2\pi)^d} \int d^d p \frac{\sin(\mathbf{p} \cdot \mathbf{b})}{s - [r_T(1-c) + r_C] \sum_{\mathbf{b}} (e^{i\mathbf{p} \cdot \mathbf{b}} - 1)} = 0 \quad (\text{C.14})$$

for the lattices considered herein. The expression above follows, for instance, by explicit calculations for each of the lattices using the trigonometric identities [33]

$$\begin{aligned} \sin(z_1 + z_2) &= \sin(z_1) \cos(z_2) + \cos(z_1) \sin(z_2), \\ \cos(z_1 + z_2) &= \cos(z_1) \cos(z_2) - \sin(z_1) \sin(z_2), \end{aligned} \quad (\text{C.15})$$

and (using the expressions above)

$$\begin{aligned} \sin(z_1 + z_2 + z_3) &= -\sin(z_1) \sin(z_2) \sin(z_3) + \sin(z_1) \cos(z_2) \cos(z_3) \\ &\quad + \cos(z_1) \sin(z_2) \cos(z_3) + \cos(z_1) \cos(z_2) \sin(z_3) \end{aligned} \quad (\text{C.16})$$

$$\begin{aligned} \cos(z_1 + z_2 + z_3) &= \cos(z_1) \cos(z_2) \cos(z_3) - \cos(z_1) \sin(z_2) \sin(z_3) \\ &\quad - \sin(z_1) \sin(z_2) \cos(z_3) - \sin(z_1) \cos(z_2) \sin(z_3) \end{aligned} \quad (\text{C.17})$$

as well as the fact that ( $v = x, y, z$  and  $\alpha, \beta$  are arbitrary real numbers)

$$\int_{-\pi/l_v}^{\pi/l_v} \frac{dp_v}{2\pi} \frac{\sin(\alpha p_v) \cos(\beta p_v)}{s - [r_T(1-c) + r_C] \sum_{\mathbf{b}} (e^{i\mathbf{p} \cdot \mathbf{b}} - 1)} = 0, \quad (\text{C.18})$$

and

$$\int_{-\pi/l_v}^{\pi/l_v} \frac{dp_v}{2\pi} \frac{\sin(\alpha p_v)}{s - [r_T(1-c) + r_C] \sum_{\mathbf{b}} (e^{i\mathbf{p} \cdot \mathbf{b}} - 1)} = 0. \quad (\text{C.19})$$

These results follow, since the denominators above are invariant under  $p_x \rightarrow -p_x$ ,  $p_y \rightarrow -p_y$  and  $p_z \rightarrow -p_z$  for all lattices herein.

To proceed we write  $\mathbf{b} = \pm a\mathbf{v}$  (c.f. Table 2), in Eq. (C.12) and Eq. (C.11). We also use the fact that for all lattices considered we have

$$\sum_{\mathbf{v}} (\mathbf{q} \cdot \mathbf{v}) R(a\mathbf{v}', a\mathbf{v}, s) = (\mathbf{q} \cdot \mathbf{v}') V(s) \quad (\text{C.20})$$

where the quantity  $V(s)$  depends on the lattice (see below). The expressions for  $V(s)$  are calculated explicitly for each lattice by using Eq. (C.15) to Eq. (C.18). We then obtain the results for  $V(s)$  as given in the main text, after a change of integration variables  $p_x \rightarrow p_x/l_x$ ,  $p_y \rightarrow p_y/l_y$  and  $p_z \rightarrow p_z/l_z$ . By combining Eq. (C.20) and Eq. (C.11), we get a closed form equation for  $G(s)$ :

$$G(s) = 4a^2 V(s) \sum_{\mathbf{v}} (\mathbf{q} \cdot \mathbf{v})^2 + 2[r_T(1-3c) + r_C] V(s) G(s), \quad (\text{C.21})$$

Finally, solving the equation above, and using the explicit nearest neighbour vectors listed in Table 1, we arrive at:

$$G(s) = \frac{2a^2 n_b V(s) |\mathbf{q}|^2 / d}{1 - 2[r_T(1-3c) + r_C] V(s)}. \quad (\text{C.22})$$

where  $|\mathbf{q}|^2 = q_x^2 + q_y^2 + q_z^2$  for 3D lattices,  $|\mathbf{q}|^2 = q_x^2 + q_y^2$  for 2D lattices and  $|\mathbf{q}|^2 = q_x^2$  for 1D lattices. Above,  $n_b$  and  $d$  are the number of neighbouring sites and the lattice dimension, respectively.

## Appendix D. First order correlation factor: time dependence and long time limit

We detail here the derivation of the first order results for the correlation factor, Eqs. (51) and (52), respectively, for a linear (one-dimensional) lattice and for higher-dimensional lattices.

*One-dimensional lattice:* For a linear lattice the integral  $V(s)$ , given in Eq. (46), can be evaluated:

$$\begin{aligned} V(s) &= \frac{1}{2\pi} \int_{-\pi}^{\pi} dp \frac{\sin^2(p)}{s - w\lambda(p)} = \frac{1}{4w^2} \left( s + 2w - \sqrt{s(s+4w)} \right) \\ &= \frac{1}{s + 2w + \sqrt{s(s+4w)}}, \end{aligned} \quad (\text{D.1})$$

where  $\lambda(p) = 2(\cos p - 1)$  and  $w = r_C + r_T(1 - c)$ . Eq. (45) becomes

$$A_1(t)t = -4n_b a^2 L^{-1} \left\{ \frac{1}{s^2} \frac{1}{s + 2b + \sqrt{s(s+4w)}} \right\}, \quad (\text{D.2})$$

with  $b = 2r_{TC}$ . Focusing on the long-time limit ( $s \rightarrow 0$ ) we find, after inversion back to the time-domain, that:

$$A_1(t) \underset{t \rightarrow \infty}{\sim} \frac{A_0}{\gamma^2} \left( -1 + \frac{1}{c} \sqrt{\frac{r+1-c}{r_T \pi t}} + O(t^{-1}) \right), \quad (\text{D.3})$$

where  $A_0$  is given in Eq. (43) and  $\gamma^2$  is defined in Eq. (29). Inserting the expression above into Eq. (49) yields Eq. (51) in the main text.

*Two- and three-dimensional lattices:* In the higher-dimensional lattices ( $d \geq 2$ ) the integral  $V(s)$ , given in Eqs. (46), (47) and (48) cannot be evaluated. However, the long time behavior may still be derived. Considering the asymptotic behavior of Eq. (45) we have

$$A_1(t)t \underset{t \rightarrow \infty}{\sim} L^{-1} \left\{ \frac{1}{s^2} \frac{-4n_b a^2 V(0)}{1 - 2(r_T(1 - 3c) + r_C)V(0)} \right\}, \quad (\text{D.4})$$

Hence, if we define  $\beta$  through  $(\beta + 1)^{-1} = 2r_T(r + 1 - c)V(0)$ , we arrive at

$$A_1(t) \underset{t \rightarrow \infty}{\sim} -\frac{A_0}{\gamma^2} \left( \frac{2c}{2c + (r + 1 - c)\beta} \right), \quad (\text{D.5})$$

which yields Eq. (52) in the main text. Using Eq. (46), Eq. (47) and Eq. (48) we get the explicit expressions for  $\beta$  according to

$$(\beta_{\text{hyp}} + 1)^{-1} = \int_{-\pi}^{\pi} \frac{dp_x}{2\pi} \int_{-\pi}^{\pi} \frac{dp_y}{2\pi} \int_{-\pi}^{\pi} \frac{dp_z}{2\pi} \frac{\sin^2(p_x)}{\sum_{\mathbf{v}} (1 - \cos(\mathbf{p} \cdot \mathbf{v}))}, \quad (\text{D.6})$$

$$(\beta_{\text{bcc}} + 1)^{-1} = 4 \int_{-\pi}^{\pi} \frac{dp_x}{2\pi} \int_{-\pi}^{\pi} \frac{dp_y}{2\pi} \int_{-\pi}^{\pi} \frac{dp_z}{2\pi} \frac{\sin^2(p_x/\sqrt{3}) \cos^2(p_y/\sqrt{3}) \cos^2(p_z/\sqrt{3})}{\sum_{\mathbf{v}} (1 - \cos(\mathbf{p} \cdot \mathbf{v}))}, \quad (\text{D.7})$$

$$(\beta_{\text{fcc}} + 1)^{-1} = 2 \int_{-\pi}^{\pi} \frac{dp_x}{2\pi} \int_{-\pi}^{\pi} \frac{dp_y}{2\pi} \int_{-\pi}^{\pi} \frac{dp_z}{2\pi} \frac{\sin^2(p_x/\sqrt{2}) \cos(p_y/\sqrt{2}) (\cos(p_y/\sqrt{2}) + \cos(p_z/\sqrt{2}))}{\sum_{\mathbf{v}} (1 - \cos(\mathbf{p} \cdot \mathbf{v}))}. \quad (\text{D.8})$$

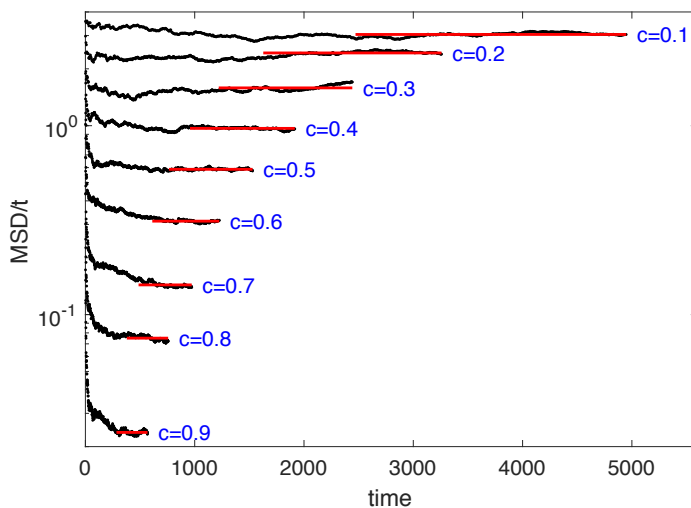


**Figure E1.** Example of MSD fits to simulation data.  $MSD(t)/t$  (logarithmic scale) as a function of time for a square lattice with  $r = 1/20$  for different concentrations  $c$  as indicated. The black marks represent the result from the simulation, whereas the red lines indicate the outcome of the fitting procedure as well as the range of data for which the fitting procedure was applied, see Eq. (E.2).

For square lattices the two-dimensional integral for  $\beta_{\text{hyp}}$  can be evaluated exactly as  $\beta_{\text{square}} = 2/(\pi - 2)$ , whereas for the three-dimensional lattices the integrals above are numerically calculated, see Table 2.

### Appendix E. Fitting procedure for the diffusion constant

From the set of trajectories generated using the algorithm from Sec. 4.1, we calculate squared displacements  $y_i^{(m)}$ , where  $m$  ( $1 \leq m \leq M$ ) labels trajectories and  $i$  labels sampling times ( $i \in [1, n_s]$ ,  $n_s$  being the number of sampling times). The estimated MSD then is

$$\bar{y}_i = \frac{1}{M} \sum_{m=1}^M y_i^{(m)}. \quad (\text{E.1})$$

We are here interested in the long-time behavior of the MSD. To that end, we keep only data from sampling times for which  $t > t_{\text{min}}$  with:

$$t_{\text{min}} = \frac{10}{c \min(r_C, r_T)}. \quad (\text{E.2})$$

To fit the MSD we used  $\chi^2$  regression for uncorrelated data [34]. We have for the estimated diffusion constant  $\hat{D}$ :

$$\hat{D} = \frac{1}{2d} \frac{\sum_i \bar{y}_i t_i / \bar{\sigma}_i^2}{\sum_i t_i^2 / \bar{\sigma}_i^2} \quad (\text{E.3})$$

with

$$\bar{\sigma}_i^2 = \frac{1}{M(M-1)} \sum_{m=1}^M (y_i^{(m)} - \bar{y}_i)^2, \quad (\text{E.4})$$

the variance of  $\bar{y}_i$ . For all fits we used  $n_s = 10^{-1}M$  equidistant sampling times. In Fig. E1 we show a few examples of fits, here for the data corresponding to Fig. 3 (upper panel, blue marks).

## References

- [1] Haus J and Kehr K 1987 *Phys. Rep.* **150** 263–406
- [2] Havlin S and Ben-Avraham D 1987 *Adv. Phys.* **36** 695–798
- [3] Dean D S and Lefèvre A 2004 *Phys. Rev. E* **69** 061111
- [4] Bouchaud J P and Georges A 1990 *Phys. Rep.* **195** 127–293
- [5] Burlatsky S, Oshanin G, Mogutov A and Moreau M 1992 *Phys. Lett. A* **166** 230–234
- [6] Bénichou O, Cazabat A M, Lemarchand A, Moreau M and Oshanin G 1998 *J. Stat. Phys.* **97** 351–371
- [7] Illien P, Bénichou O, Mejía-Monasterio C, Oshanin G and Voituriez R 2013 *Phys. Rev. Lett.* **111** 038102
- [8] Bénichou O, Bodrova A, Chakraborty D, Illien P, Law A, Mejía-Monasterio C, Oshanin G and Voituriez R 2013 *Phys. Rev. Lett.* **111** 260601
- [9] Kundu A and Cividini J 2016 *EPL* **115** 54003
- [10] Bénichou O, Illien P, Oshanin G, Sarracino A and Voituriez R 2015 *Phys. Rev. Lett.* **115** 220601
- [11] Kikuchi R and Sato H 1970 *J. Chem. Phys.* **53** 2702–2713
- [12] Sankey O F and Fedders P A 1979 *Phys. Rev. B* **20** 39–45
- [13] Bender O and Schroeder K 1979 *Phys. Rev. B* **19** 3399–3413
- [14] Fedders P A and Sankey O F 1977 *Phys. Rev. B* **15** 3580–3585
- [15] Nakazato K and Kitahara K 1980 *Prog. Theor. Phys.* **64** 2261–2264
- [16] Brummelhuis M and Hilhorst H 1989 *Phys. A Stat. Mech. its Appl.* **156** 575–598
- [17] Tahir-Kheli R A and Elliott R J 1983 *Phys. Rev. B* **27** 844–857
- [18] van Beijeren H and Kutner R 1985 *Phys. Rev. Lett.* **55** 238–241
- [19] Benichou O, Klafter J, Moreau M and Oshanin G 2000 *Phys. Rev. E* **62** 3327–39
- [20] Bénichou O and Oshanin G 2002 *Phys. Rev. E* **66** 031101
- [21] Bénichou O, Klafter J, Moreau M and Oshanin G 2005 *Chem. Phys.* **319** 16–27
- [22] Bénichou O, Illien P, Oshanin G, Sarracino A and Voituriez R 2014 *Phys. Rev. Lett.* **113** 268002
- [23] Bénichou O, Illien P, Oshanin G, Sarracino A and Voituriez R 2016 *Phys. Rev. E* **93** 032128
- [24] Lang I G and Firsov Y A 1963 *Sov. Phys. JETP* **16** 1301
- [25] Mahan G D 2013 *Many-Particle Physics* Physics of Solids and Liquids (Springer Science & Business Media)
- [26] Suzuki Y, Kitahara K, Fujitani Y and Kinouchi S 2002 *J. Phys. Soc. Japan* **71** 2936–2943
- [27] Harris T E 1965 *J. Appl. Probab.* **2** 323
- [28] Gonçalves P and Jara M 2008 *J. Stat. Phys.* **132** 1135–1143
- [29] Ambjörnsson T, Lizana L, Lomholt M A and Silbey R J 2008 *J. Chem. Phys.* **129** 185106
- [30] Bebbington A C 1975 *Appl. Stat.* **24** 136
- [31] GNU General Public License accessed: 2007-06-29 URL <http://www.gnu.org/licenses/gpl.html>
- [32] Wilcox R M 1967 *J. Math. Phys.* **8** 962–982
- [33] Abramowitz M and Stegun I 1964 *Handbook of Mathematical Functions: With Formulas, Graphs, and Mathematical Tables* Applied mathematics series (Dover Publications)
- [34] Press W H, Teukolsky S A, Vetterling W T and Flannery B P 2007 *Numerical Recipes 3rd Edition: The Art of Scientific Computing* (Cambridge University Press)